International Immunopharmacology 126 (2024) 111289

Contents lists available at ScienceDirect

International Immunopharmacology

journal homepage: www.elsevier.com/locate/intimp

Mirabegron, dependent on β3-adrenergic receptor, alleviates mercuric chloride-induced kidney injury by reversing the impact on the inflammatory network, M1/M2 macrophages, and claudin-2

Mahmoud M. Kamal [a], Hanan S. El-Abhar [b], Dalaal M. Abdallah [c,*], Kawkab A. Ahmed [d], Nour Eldin S. Aly [a], Mostafa A Rabie [c,e]

[a] Research Institute of Medical Entomology, General Organization for Teaching Hospitals and Institutes, Cairo, Egypt
[b] Department of Pharmacology, Toxicology, and Biochemistry, Faculty of Pharmacy, Future University in Egypt (FUE), 11835 Cairo, Egypt
[c] Pharmacology and Toxicology Department, Faculty of Pharmacy, Cairo University, 11562 Cairo, Egypt
[d] Pathology Department, Faculty of Veterinary Medicine, Cairo University, Cairo, Egypt
[e] Faculty of Pharmacy and Drug Technology, Egyptian Chinese University (ECU), 19346, Egypt

ARTICLE INFO

Keywords:
AKI
IL-4 & IL-13
STAT-6
IL-17
PI3K
ERK½, PPAR-α, NF-κB
miRNA-127
HNF-4α
HNF-1α

ABSTRACT

The β3-adrenergic receptor (β3-AR) agonism mirabegron is used to treat overactive urinary bladder syndrome; however, its role against acute kidney injury (AKI) is not unveiled, hence, we aim to repurpose mirabegron in the treatment of mercuric chloride ($HgCl_2$)-induced AKI. Rats were allocated into normal, normal + mirabegron, $HgCl_2$ untreated, $HgCl_2$ + mirabegron, and $HgCl_2$ + the β3-AR blocker SR59230A + mirabegron. The latter increased the mRNA of β3-AR and miR-127 besides downregulating NF-κB p65 protein expression and the contents of its downstream targets iNOS, IL-4, -13, and -17 but increased that of IL-10 to attest its anti-inflammatory capacity. Besides, mirabegron downregulated the protein expression of STAT-6, PI3K, and $ERK_{1/2}$, the downstream targets of the above cytokines. Additionally, it enhanced the transcription factor PPAR-α but turned off the harmful hub HNF-4α/HNF-1α and the lipid peroxide marker MDA. Mirabegron also down-regulated the CD-163 protein expression, which besides the inhibited correlated cytokines of M1 (NF-κB p65, iNOS, IL-17) and M2 (IL-4, IL-13, CD163, STAT6, $ERK_{1/2}$), inactivated the macrophage phenotypes. The crosstalk between these parameters was echoed in the maintenance of claudin-2, kidney function-related early (cystatin-C, KIM-1, NGAL), and late (creatinine, BUN) injury markers, besides recovering the microscopic structures. Nonetheless, the pre-administration of SR59230A has nullified the beneficial effects of mirabegron on the aforementioned parameters. Here we verified that mirabegron can be repurposed to treat $HgCl_2$-induced AKI by activating the β3-AR. Mirabegron signified its effect by inhibiting inflammation, oxidative stress, and the activated M1/M2 macrophages, events that preserved the proximal tubular tight junction claudin-2 via the intersection of several trajectories.

1. Introduction

Mercury is one of the main environmental pollutants that despite being ubiquitously used in medicine, industry, and agriculture distributes in ecosystems and is imperishable [1]. Mercury is present in different forms chemically, where it can exist as an elemental mercury, as well as inorganic and organic mercury compounds [1]. The kidney is the primary target organ susceptible to inorganic mercury, particularly mercuric chloride ($HgCl_2$). In this context, mercury accumulates within the proximal tubules eliciting nephrotoxicity [2]. Mercuric ions stimulate the generation of significant quantities of reactive oxygen species (ROS) and inflammatory cytokines in the kidney by activating nuclear

Abbreviations: BUN, blood urea nitrogen; ERK½, extracellular signal-regulated kinase one & two; $HgCl_2$, mercuric chloride; HNF-1α, hepatocyte nuclear factor-1α; HNF-4 α, hepatocyte nuclear factor-4α; PI3K, phosphatidylinositol 3-kinase; IL-, interleukin-(4, 13, 17); iNOS, inducible nitric oxide synthase; KIM-1, kidney injury molecule-1; MDA, malondialdehyde; NF-κB p65, nuclear factor-κB p65; NGAL, neutrophil gelatinase-associated lipocalin; PPAR- α, peroxisome proliferator-activated receptor- α; SR, SR 59230A, a selective beta −3 adrenergic receptor antagonist; STAT-6, signal transducer and activator of transcription − 6.

* Corresponding author.
E-mail address: dalaal.abdallah@pharma.cu.edu.eg (D.M. Abdallah).

https://doi.org/10.1016/j.intimp.2023.111289
Received 12 July 2023; Received in revised form 21 November 2023; Accepted 22 November 2023
Available online 27 November 2023

factor (NF)-κB p65, the parent transcription factor [3].

In a previous study, $HgCl_2$-induced tubular injury was accompanied by infiltration of mononuclear cells with macrophages being the most predominant population [4]. Of note, macrophages play a pivotal role in kidney homeostasis, and their phenotyping is under dynamic control to actively participate in immune surveillance and tissue repair. In response to various stimuli, these immune cells modulate inflammation and contribute to the delicate balance of renal function [5,6]. Indeed, macrophages are incriminated in either launching an inflammatory response or triggering signaling pathways to insulted epithelial cells to induce their proliferation/repair or avert fibrosis [7]. The activated M1 macrophages are accused of exploiting pro-inflammatory cytokines and ROS. This triggers a consequent anti-inflammatory phase that limits damage *via* polarizing M1 macrophages into the alternatively M2-activated ones to suppress inflammation and aid tissue remodeling [8]. Notably, these M2 macrophages are predominantly detected in the renal interstitium during the repairing phase of acute tubular injury [7].

Further pathomechanisms by which different toxins cause kidney injury is the alteration of tight junctions (TJs), which are vital subcellular moieties that play a critical role in the function of the epithelial barrier hence affecting kidney homeostasis [9]. Indeed, claudin, an essential element of TJs, forms a paracellular transport passage for the reabsorption of different ions in the kidney [10]. The enhanced expression of claudin-2 protects the kidney by minimizing the energy consumed during the transport processes [11]. On the other hand, defects in claudin function were reported in animal kidney injury models, including obstructive nephropathy-induced fibrosis, as well as cisplatin-, cadmium (Cd^{2+})-, and diabetic-induced nephrotoxicity [10,12].

Apart from the role of the above molecules, the kidney not only serves as a target for the sympathetic nervous system (SNS) but also emits signals that influence the activity of this system [13]. The SNS has a great influence on kidney function through the modulation of several adrenergic receptors (ARs) [13], however, the role of the activated β-3 adrenoreceptor (β3-AR) in the kidney is not conclusive so far [14,15]. This third isoform of the ARs is located peripherally on different organs including kidney tubules besides the adipose tissue, gastrointestinal tract, urinary bladder, and cardiovascular system [16].

Targeting the pharmacological actions of this receptor, the β3-AR agonist mirabegron has been approved worldwide for treating patients with overactive urinary bladder (OUB) syndrome; nevertheless, the extra-bladder off-target effects were reported in cases of heart failure and metabolic disease [17]. Recently, we tested the repurposing of mirabegron against an ulcerative colitis model and showed its ability to alleviate colitic injury by its antioxidant, anti-fibrotic, and anti-inflammatory characteristics through modulating several hubs, such as presenilin and NOTCH signaling as well as NF-κB p65/TNF-α [18]. Besides, mirabegron inhibited the lipopolysaccharide/toll-like receptor-4 pathway and the NADPH oxidase/catalase reducing the overly produced ROS and pro-inflammatory mediators in human macrophages [19].

Based on the previous literature, we investigated the potential nephron-therapeutic effect of mirabegron against $HgCl_2$-induced acute kidney injury (AKI). We also evaluated whether the inhibition of β3-receptor using the selective blocker SR 59230A can modulate the inflammatory transcription factor NF-κB p65, its upstream activators, and the downstream targets, besides miR-127, macrophage phenotyping, and kidney barrier.

2. Material and methods

2.1. Animals and Ethics statement

Male Wistar rats, with a weight ranging between 180 and 200 g, were used in this work (Faculty of Pharmacy, Cairo University, Cairo, Egypt) and were fed a standard chow diet and permitted water *ad libitum*. Animals were kept in an environment of a constant temperature (23 ± 2 °C), humidity (60 ± 10 %), and an equal period of dark/light cycle.

The investigation protocol was approved by the Ethics Research Committee of the Faculty of Pharmacy, Cairo University (PT 2546) and conforms to the Guide for the Care and Use of Laboratory Animals (NIH publication No. 8023, revised 2011). The animal suffering was carefully minimized during the experiment.

2.2. Induction of $HgCl_2$ renal toxicity

To induce AKI, 3 mg/kg of $HgCl_2$ (Sigma-Aldrich, MO, USA) [20] was liquified in saline to be injected with a single subcutaneous injection.

2.3. Experimental design and sample collection

Animals were allocated into five groups (n = 9/group) and those in the first 2 groups were gavaged orally normal saline or mirabegron (Mira; 30 mg/kg) [21] to respectively serve as the control (Cont.) groups. In the following 3 groups, rats were injected with $HgCl_2$, where one group was left untreated to be nominated as the $HgCl_2$ control group (3rd group), whereas the other two groups were administered Mira 1 and 24 h after the injection of $HgCl_2$ ($HgCl_2$ + Mira group) or injected intraperitoneally with 5 mg/kg of the β3-AR blocker SR59230 A (Sigma-Aldrich, MO, USA) [22,23] 15 min before the administration of Mira to be designated as the $HgCL_2$ + SR59230 + Mira group.

One day after the last treatments, a mixture of ketamine/xylazine [100/10 mg/kg; i.p.] was used to anesthetize the animals, and blood samples were drained from the tail vein to separate sera for the measurement of kidney function parameters. Afterward, rats were sacrificed by cervical dislocation, and the kidneys of 6 rats/group were stored at − 80 °C. The right kidneys of 3 rats per group were used for western blot analysis after immersing into RIPA lysis and extraction buffer provided with a cocktail of phosphatase and protease inhibitors, whereas the other 3 right ones were submerged in RNA lysis solution and used for qRT-PCR analysis. The left kidneys of these rats (n = 6) were homogenized in ice-cold saline for the ELISA analysis. The kidneys of the remaining 3 rats per group were fixed in 10 % formalin to examine histopathological alterations and immunohistochemical assessment of CD-163 and NF-κB p65.

2.4. Renal function assessment

The colorimetric assay of creatinine and BUN was carried out in the separated sera using commercial kits (EGY-CHEM, EG, cat# CRE106100 and URE118100, respectively). In parallel, serum levels of cystatin C (cat# MBS763996), kidney injury molecule (KIM)-1 (cat# MBS355395), and neutrophil gelatinase-associated lipocalin (NGAL; cat# MBS2504748) were determined using rat ELISA kits purchased from MyBioSource (CA, USA). All experiments were processed according to the manufacturers' instructions.

2.5. Determination of renal contents of IL-4, IL-13, IL-17, IL-10, PPAR-α, STAT-6, and claudin-2 using ELISA technique

MyBioSource ELISA kits (CA, USA) were used for the determination of the protein contents of IL-13 (cat# MBS355408), IL −17 (cat# MBS164772), IL-10 (cat#MBS764911), PPAR-α (cat# MBS2504779), and STAT6 (cat# MBS454981). The ELISA kit obtained from antibodies-online GmbH (AC, DE; cat# ABIN6954827) was used to determine claudin-2 and that procured from Elabscience (TX, USA, cat# E-EL-R0014) was adopted for the quantification of IL-4. All assessments were normalized to their protein content measured by the Bradford method [24]. Additionally, the colorimetric assay kit of malondialdehyde (MDA) was purchased from Biodiagnostic (Giza, EG) and all examinations were performed according to the manufacturers' prescripts.

2.6. Analysis of renal protein expression of PI3K, HNF-1α, HNF-4α, iNOS, and $ERK_{1/2}$ using western blot

The protein extraction kit (Millipore, MA, USA; cat#: 2140) was used for quantitative renal protein analysis; samples with equal protein concentrations were loaded onto and separated by SDS-PAGE. The blots were then transferred to the PVDF membrane which was blocked with 5 % BSA and incubated with anti-p38 PI3K polyclonal antibody (1:1000; cat#: PA5-37820), anti-HNF-1α polyclonal antibody (1:500; cat#: 22426–1-AP), anti-HNF-4α monoclonal antibody (1:1000; cat#: MA1-199), anti-iNOS polyclonal antibody (1:2000; cat#: PA1-036), anti-$ERK_{1/2}$ monoclonal antibody (1:1000; cat#: 13–8600), or anti-β-actin monoclonal antibody (1:5000; cat# MA1-140) purchased from ThermoFisher Scientific Co. (MA, USA) overnight at 4 °C on a roller shaker. Following washing, membranes were subsequently probed with horseradish peroxidase-conjugated goat anti-rabbit immunoglobulin (1:1000; Dianova, HH, DE) for 1 h at room temperature. Chemiluminescence detection was performed with an Amersham detection kit (Amersham Biosciences, IL, USA) following the manufacturer's protocol and exposed to X-ray film. The densitometric analysis of the autoradiograms was used to quantify the protein with the aid of a scanning laser densitometer (GS-800 system, Bio-Rad, CA, USA). Results were expressed as arbitrary units (AU) after normalization to β-actin protein expression.

2.7. Analysis of renal mRNA expression of miR-127 and β3-AR using qRT-PCR technique

The RNeasy mini kit (Qiagen, Venlo, NL) was used to extract total RNA, and the pureness of the gained RNA was confirmed spectrophotometrically at 260/280 nm, and a matched amount of the extracted RNA was reverse transcribed into cDNA using RT-PCR kit (Promega, LEI, NL). As designed by the manufacturer, SYBR Green Master Mix (Applied Biosystems, CA, USA) was used to fulfill the quantitative RT-PCR. In a 25 μl reaction volume, cDNA (5 μl) was mixed with SYBR Green mixture (12.5 μl), RNase-free water (5.5 μl), and 2 μl of the specific primers (Table 1). The PCR settings were denaturation (95 °C for 15 sec), annealing (60 °C for 60 sec), and extension (72 °C for 60 sec) for 40 cycles. The relative expression of target genes was normalized to β-actin for the relative expression of β3-AR and to U6 for the relative expression of miR-127 using the $2^{-\Delta\Delta\ CT}$ formula.

2.8. Histopathological investigation

The paraffinized kidney specimens were cut in sagittal sections at 5 μm thickness to be stained with Hematoxylin and Eosin (H & E) [25] for blind histopathological examination. The specimen identity remained anonymous during both capturing and analyzing images. The renal histopathological alterations were studied in five non-overlapping microscopic fields including renal cortex, corticomedullary junction, and renal medulla (n = 3) and scored from 0 to 5 according to the encompassed percent as follows: normal (0 = 0 %); mild (1= <10 %); moderate (2 = 10–25 %); severe (3 = 25–50 %); very severe (4 = 50–75 %); extensive damage (5= >75 %) [26].

Table 1
Primer sequences of target proteins used in qRT-PCR.

mRNA species	Gene ID	Primer sequence 5′-3′
miR-127	100,314,190	Forward: TAGTTTGGAGTTAGGGGTAGGGTAT Reverse: AATAAATCAAAAAAAACACCTCCAC
U6	26,826	Forward 5'-CTCGCTTCGGCAGCACA-3' Reverse 5'- AACGCTTCACGAATTTGCGT-3'
β3-AR	25,645	Forward: TAGTCCTGGTGTGGATCGTGTCCGC Reverse: GCGATGAAAACTCCGCTGGGAACTA
β-Actin	81,822	Forward: AGCCATGTACGTAGCCATCC Reverse: ACCCTCATAGATGGGCACAG

2.9. Immunohistochemical detection of protein expression of NF-κB p65 and CD-163 in the kidney

The immunoreactivity of NF–κB p65 and CD-163 was examined in the renal tissue. To the obtained sections, the primary antibodies for NF-κB p65 (1:100; cat#: SC-8008; Santa Cruz Biotechnology Inc., TX, USA) and CD-163 (1:40; cat#: 163 M−16; Cell Marque, CA, USA) were added and incubated and diaminobenzidine tetrachloride (DAB, Sigma-Aldrich, MO, USA) was then used to visualize the immune reaction. The appearance of a brown-stained cytoplasm and/or nuclei indicates the presence of positive immune reactive cells and the intensity/distribution of the brown discoloration is graded as negative (no staining), weak, moderate, or strong. In each section, positive staining was represented as the area % immune expression from 5 randomly selected fields and averaged using image analysis software (Image J, version 1.46a, NIH, Bethesda, MD, USA).

2.10. Statistical analysis

All continuous data obtained were expressed as mean ± SD and the one-way analysis of variance test (one-way ANOVA) followed by Tukey's post hoc test was adopted for the statistical analysis of these data, but the Kruskal–Wallis test followed by Dunn's multiple comparison test was used to analyze the ordinal data. Moreover, Pearson's test was used to analyze the correlation results ($p < 0.05$. GraphPad Prism software, version 9 (GraphPad Software Inc., CA, USA) was used for the statistical analysis and drawings.

3. Results

Since no significant difference was detected between the normal group treated with mirabegron (Mira) and that treated with saline (Cont.), all comparisons were related to the latter group.

3.1. Mirabegron improves renal function through activation of β3-AR in rats with $HgCl_2$-induced AKI

Relative to the Cont. group and as depicted in Fig. 1, exposure of animals to $HgCl_2$ resulted in an obvious renal dysfunction verified by elevated serum levels of (A) creatinine (7 folds) and (B) BUN (2.6 folds), as well as (C) cystatin C (1.7 folds), (D) NGAL (2.5 folds), and (E) KIM-1 (2.1 folds). Inversely, the administration of mirabegron normalized both creatinine and cystatin C and succeeded in leveling off BUN by 43 %, NGAL by 47 %, and KIM-1 by 34 %, as compared to the insult group. Nevertheless, these beneficial impacts of Mira were nullified by the pre-administration of SR 59230A, the selective β3-AR antagonist.

3.2. Mirabegron upregulates the mRNA expression of β3-AR and miR-127 in rats with $HgCl_2$-induced AKI

The administration of $HgCl_2$ (Fig. 2) has depleted the mRNA expression of (A) β3-AR to nearly one-fifth of its Cont. value and sharply downregulated (B) miR-127 to 17 % as compared to the Cont. group. Contrariwise, mirabegron succeeded in upregulating both β3-AR (3.7 folds) and miR-127 (4.7 folds) relative to the $HgCl_2$-exposed rats, effects that were abolished by the prior administration of the β3-AR antagonist to reach a non-significant level to those of AKI.

3.3. Mirabegron signifies its anti-inflammatory capacity by inhibiting the NF-κB p65/iNOS axis in rats with $HgCl_2$-induced AKI

As depicted in Fig. 3, the section of (B) mirabegron reveals negative NF-κB p65 expression to mimic that of (A) the Cont. group. However, (C) $HgCl_2$-induced AKI markedly intensified the renal immunoreactivity of NF-κB p65 to be canceled upon the post-administration of (D) mirabegron. To verify the role of β3-AR, the section of (E) mirabegron preceded

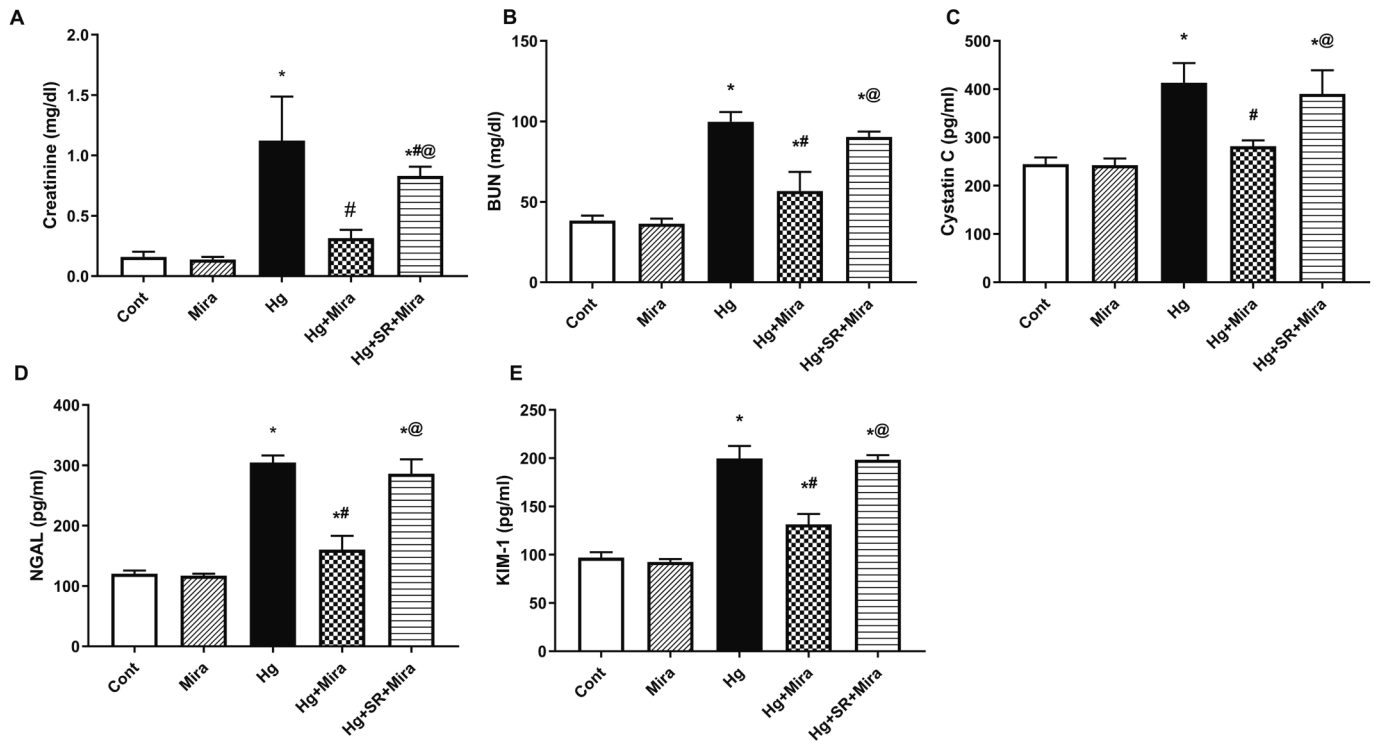

Fig. 1. Effect of Mira with or without SR59230A on serum levels of (A) creatinine, (B) BUN, (C) cystatin C, (D) NGAL, and (E) KIM-1 in $HgCl_2$-induced AKI in rats. Results are presented as means ± SD (n = 6) and the one-way ANOVA followed by Tukey's Multiple Comparison tests was adopted to analyze the data statistically. As compared to the Cont. (*), Hg ($^{\#}$), and Hg + Mira ($^{@}$)-treated group ($p < 0.05$). Mira was administered orally 1 and 24 hrs. after $HgCl_2$ subcutaneous injection, whereas the selective β3-AR blocker SR59230A was administered intraperitoneally 15 min. before each dose of Mira. β3-AR: beta 3 adrenergic receptor; BUN: blood urea nitrogen; Cont.: control, Hg: mercuric chloride; KIM-1: kidney injury molecule-1; Mira: mirabegron; NGAL: neutrophil gelatinase-associated lipocalin; SR: SR59230A, a selective β3-AR antagonist.

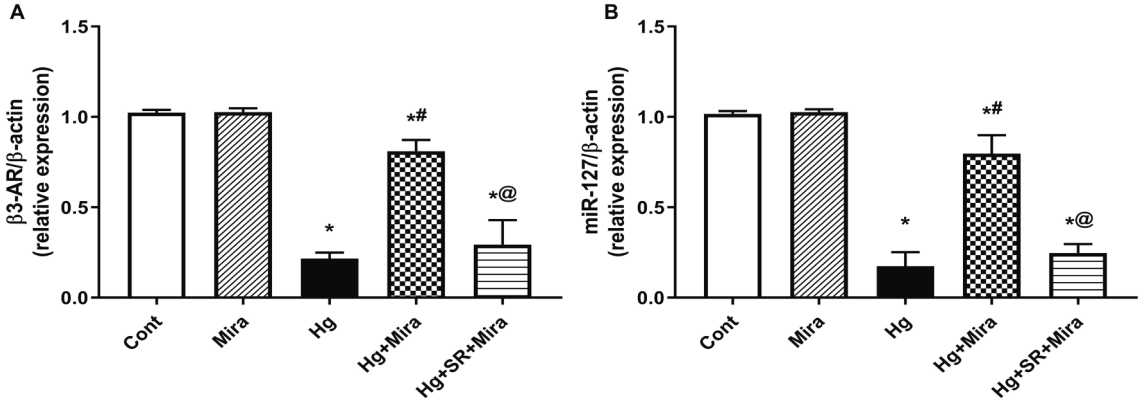

Fig. 2. Effect of Mira with or without SR59230A on the expression of (A) β3-AR, and (B) miR-127 in HgCl2-induced AKI in rats. Results are presented as means ± SD (n = 6). One-way ANOVA followed by Tukey's Multiple Comparison tests was adopted to analyze the data statistically. As compared to Cont. (*), Hg ($^{\#}$), and Hg + Mira ($^{@}$)-treated group ($p < 0.05$). Mira was administered orally 1 and 24 hrs. after $HgCl_2$ subcutaneous injection, whereas the selective β3-AR blocker SR59230A was administered intraperitoneally 15 min. before each dose of Mira. β3-AR: beta 3 adrenergic receptor; Cont.: control, Hg: mercuric chloride; Mira: mirabegron; SR: SR59230A, a selective β3-AR antagonist.

by SR59230A re-intensified the protein expression of NF-κB p65. All these effects are summarized in panel F, where $HgCl_2$ caused a 52.8-fold increase in NF-κB p65, whereas treatment with mirabegron leveled off its expression by 81 %, an effect that was nullified in the blocker-treated group. In the same pattern, (G) the protein expression of iNOS, a downstream target of NF-κB p65, was markedly boosted (4.7 folds), whereas treatment with mirabegron was able to downregulate this expression to 42 %, but in the presence of SR59230A, the iNOS expression was enhanced to imitate the effect of $HgCl_2$.

3.4. Mirabegron inhibits inflammatory cytokines and their downstream targets in rats with $HgCl_2$-induced AKI

Fig. 4 reveals that relative to the Cont. group, the insult bolstered (A) IL-4 (2.3 folds) and (B) IL-13 (3.4 folds), as well as their downstream regulatory protein (C) STAT-6 (2.7 folds) but halved the anti-inflammatory cytokine (D) IL-10. Mirabegron, on the other hand, hindered the effect of $HgCl_2$ by leveling off IL-4, IL-13, and STAT-6 but increased that of IL-10 to 2.1-fold compared to the $HgCl_2$-treated group. These effects were mediated by the activation of β3-AR since blocking

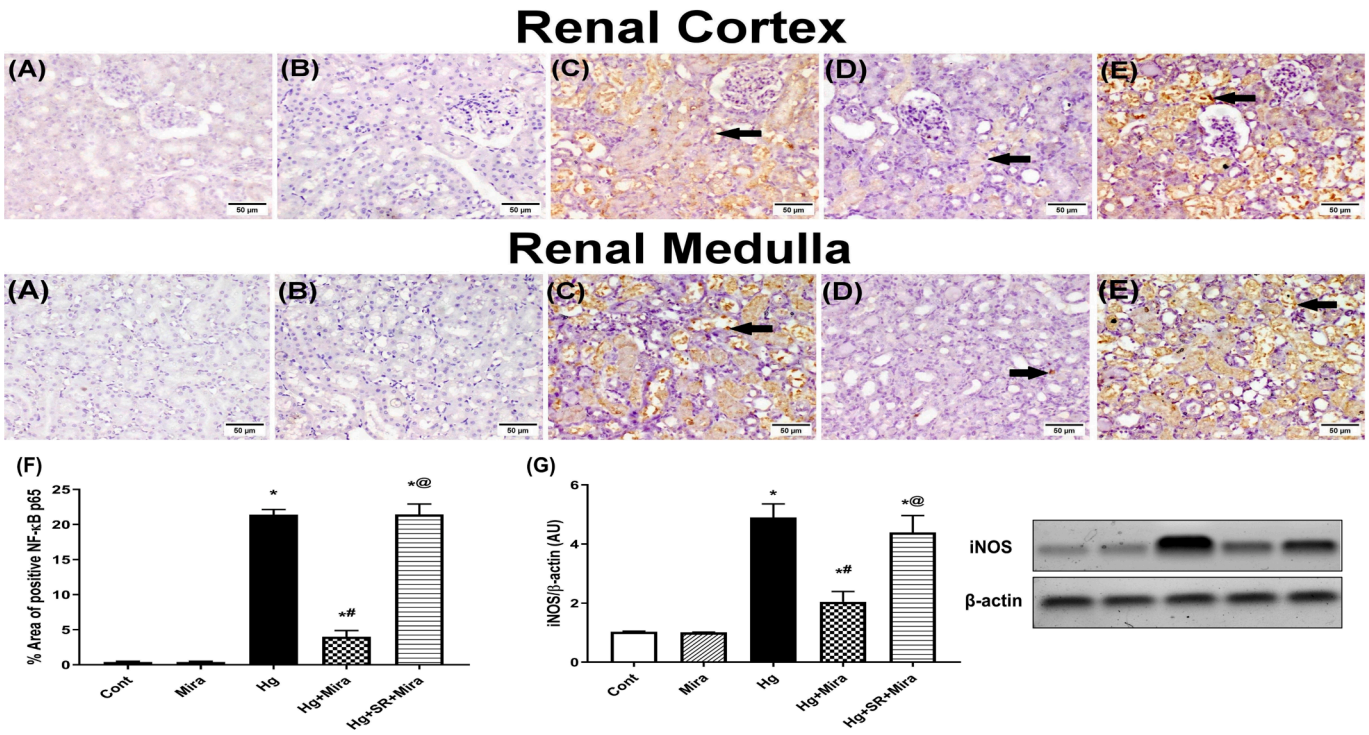

Fig. 3. Effect of Mira with or without SR59230A on renal NF-κB p65 immunoreactivity and protein expression of iNOS in $HgCl_2$-induced AKI in rats. Section of (C) $HgCl_2$ showed intense expression of NF-κB p65 relative to the null expression seen in sections of (A & B) Cont. and Mira. The expression was sharply depleted in the section of (D) $HgCl_2$ + Mira to be strengthened again in the section of (E) $HgCl_2$ + SR59230A + Mira. Panel F summarizes these data. Panel (G) duplicates the previous effects on the protein expression of iNOS. Results are presented as means ± SD (n = 3) and the one-way ANOVA followed by Tukey's Multiple Comparison tests was adopted to analyze the data statistically. As compared to Cont. (*), Hg ($^{\#}$), and Hg + Mira ($^{@}$)-treated group ($p < 0.05$). Mira was administered orally 1 and 24 hrs. after $HgCl_2$ subcutaneous injection, whereas the selective β3-AR blocker SR59230A was administered intraperitoneally 15 min. before each dose of Mira. β3-AR: beta 3 adrenergic receptor; Cont.: control, Hg: mercuric chloride; iNOS: inducible nitric oxide synthase; Mira: mirabegron; NF-κB: nuclear factor kappa B. SR: SR59230A, a selective β3-AR antagonist.

this receptor returned all parameters to almost their level in the $HgCl_2$ group. To further verify the injurious effect of $HgCl_2$, Fig. 5 shows that the nephrotoxic metal increased renal content of (A) IL-17 (2.7 folds) and its downstream targets (B) PI3K (5.8 folds) and (C) $ERK_{1/2}$ (6.3 folds) relative to the Cont. group. Contrariwise, the β3-AR agonist reduced the renal content of IL-17, as well as the protein expression of PI3K and $ERK_{1/2}$ to be upregulated once more by the β3-AR antagonist.

3.5. Mirabegron inhibits the protein expression of HNF-4α and HNF-1α in rats with $HgCl_2$-induced AKI

In Fig. 6, $HgCl_2$ extended its inflammatory event and upregulated the protein expressions of the upstream axis of NF-κB p65 (A) HNF-4α (5.3 folds) and (B) HNF-1α (6.6 folds) compared to the Cont. group. Conversely, mirabegron signified its anti-inflammatory effect by suppressing both HNF-4α and HNF-1α by around 55 % compared to the $HgCl_2$-exposed rats in a β3-AR-dependent manner. In this regard, SR 59230A successfully antagonized the mirabegron effect and doubled the expression of the transcriptional activators to replicate the effect of $HgCl_2$.

3.6. Mirabegron suppresses the phenotypic markers of macrophages M1 and M2 in rats with $HgCl_2$-induced AKI

The nephrotoxic metal triggered unexpectedly the two types of macrophages, as evidenced by the induction of both NF-κB p65 and iNOS (M1 phenotype markers) and the cytokines IL-4, IL-13, and IL-17 (M2 phenotype markers). Additionally, Fig. 7 supports the activation of the M2 phenotype by the strengthened immune expression of CD163, an indicator of M2 macrophages, in the (C) $HgCl_2$-treated group opposite to both (A) Cont. and (B) mirabegron-Cont. groups that show negative immune expression. However, post-administration of (D) mirabegron to the nephrotoxic rats divulged a weak immune expression of this factor, an effect that was canceled by the pre-administration of the (E) β3-AR blocker. All these effects are summarized in panel F.

3.7. Mirabegron reduced oxidative stress and enhanced the protein contents of PPAR-α and claudin-2 in $HgCl_2$-induced AKI

As shown in Fig. 8, $HgCl_2$ injurious effect triggered oxidative stress indicated by the 3.6-fold increase in the lipid peroxide marker (A) MDA. Moreover, the insult sharply abated the renal contents of (B) PPAR-α and the TJ (C) claudin-2 to almost one-third of the Cont. values. However, mirabegron reverted the effect of the nephrotoxic metal, where it signified its antioxidant effect by reducing MDA but augmented the nephroprotective proteins PPAR-α and claudin-2, effects that were annulled by the β3-AR antagonist.

3.8. Mirabegron improves the renal histopathological alterations induced by $HgCl_2$

As illustrated in Fig. 9, administration of (C) $HgCl_2$ altered the renal architecture in the cortex and medulla. The renal tubular lining epithelia reveal vacuolar degeneration and coagulative necrosis, besides the presence of eosinophilic renal cast in the lumen, and infiltration of inflammatory cells compared to the (A, B) control groups which show normal histoarchitecture of renal parenchyma of the glomeruli and renal tubules. However, the (D) mirabegron-treated group presents a recession of the formerly stated injuries revealing slight vacuolar degeneration of the epithelial lining and the presence of renal casts in the lumen

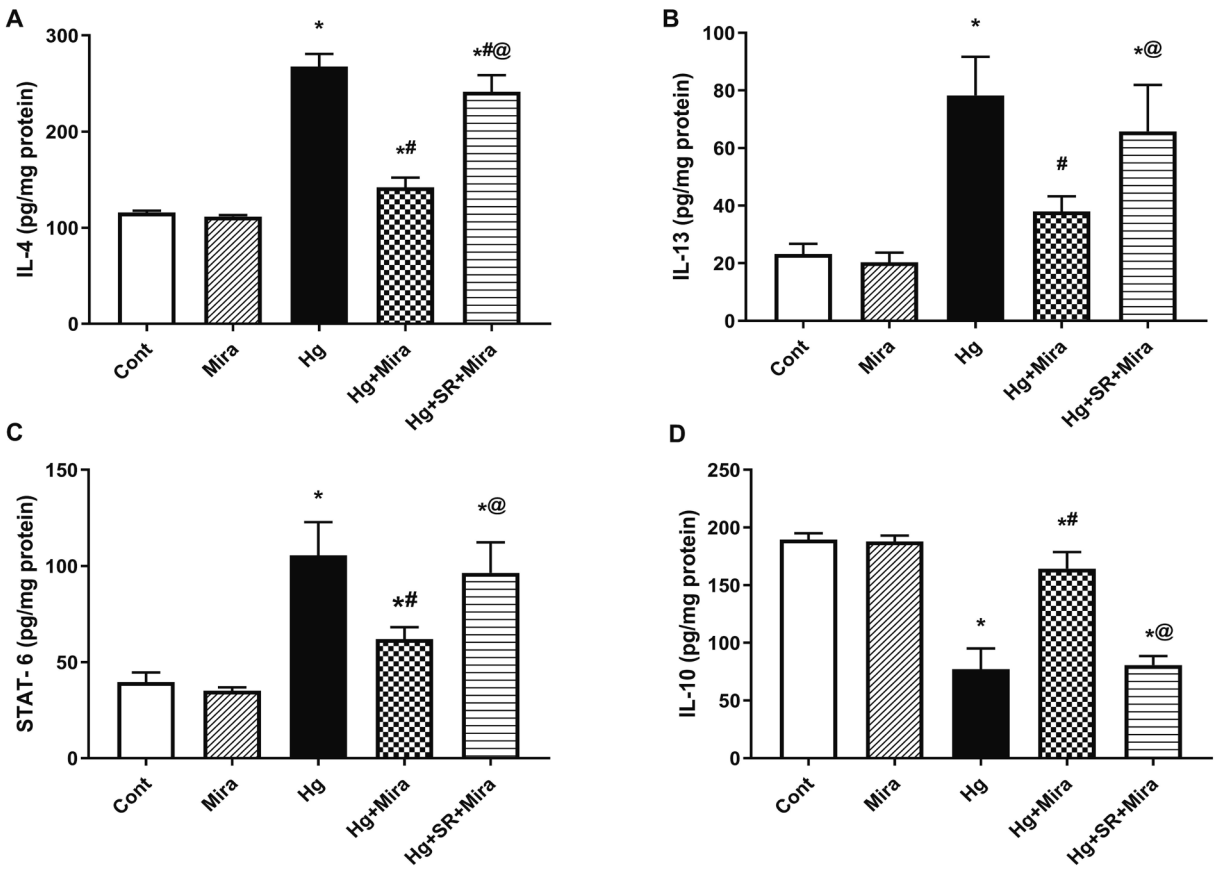

Fig. 4. Effect of Mira with or without SR59230A on renal contents of (A) IL-4, (B) IL-13, (C) STAT-6, and (D) IL-10 in $HgCl_2$-induced AKI in rats. Results are presented as means ± SD (n = 6) and the one-way ANOVA followed by Tukey's Multiple Comparison tests was adopted to analyze the data statistically. As compared to Cont. (*), Hg ($^{\#}$), and Hg + Mira ($^{@}$)-treated group ($p < 0.05$). Mira was administered orally 1 and 24 hrs. after $HgCl_2$ subcutaneous injection, whereas the selective β3-AR blocker SR59230A was administered intraperitoneally 15 min. before each dose of Mira. β3-AR: beta 3 adrenergic receptor; Cont.: control, Hg: mercuric chloride; IL-: interleukin-; Mira: mirabegron; NF-κB: nuclear factor kappa B; SR: SR59230A, a selective β3-AR antagonist; STAT-6: signal transducer and activator of transcription 6.

of some renal tubules. Such amendments were greatly reversed by the administration of (E) SR 59230A which depicts injuries in the renal tubules indicated by vacuolar degeneration and coagulative necrosis in the epithelium, renal cast in the lumen, and infiltration of inflammatory cells. Panels F and G summarize the impact of the different treatments on the collective and individual damage scoring, respectively.

3.9. Correlation analysis

Besides the documented impact of β3-AR on kidney function by using the blocker SR 59230A, Fig. 10 further supports this link, where the gene expression of this receptor displayed a high inverse correlation with (A) creatinine ($r = -0.98$, $p = 0.0025$), (B) BUN ($r = -0.99$, $p = 0.0001$), (C) cystatin-C ($r = -0.99$, $p < 0.0001$), (D) NGAL ($r = -0.99$, $p < 0.0001$), and (E) KIM-1 ($r = -0.99$, $p = 0.0003$). Moreover, to study the potential role of miR-127 on the TJ (F) claudin-2, the correlation analysis between the two parameters revealed a direct positive link ($r = 0.99$, $p < 0.0001$), wheras a strong negative correlation existed between miRNA-127 and (G) STAT-6 ($r=-0.99$, $p< 0.0001$).

4. Discussion

To the authors' knowledge, our study is the first to identify and characterize the role of β3-AR in alleviating $HgCl_2$-induced kidney injury. Mirabegron acted by its anti-inflammatory and anti-oxidant characteristics besides inactivating the macrophage phenotypes and enhancing claudin-2 to restore the leaky nature of the proximal tubules to cations and water. Mirabegron inhibited the inflammatory transcription factor NF-κB p65 and the correlated cytokines (IL-4, IL-13, IL-17) and iNOS to abrogate the inflammatory loop, as well as the activated macrophages being released by the activated M1 and M2. Additionally, mirabegron offered these effects by modulating several intersecting signaling pathways, such as IL-4/PI3K, IL-4 & IL-13/STAT-6, IL-17/$ERK_{1/2}$/NF-κB p65, and HNF-4α/HNF-1α/NF-κB p65. Indeed, mirabegron has upregulated β3-AR mRNA and miRNA-127 with the enhancement of PPAR-α to aid in the anti-inflammatory role and to improve kidney function. The pre-administration of SR 59230A has nullified such beneficial effects to confirm the role of β3-AR.

Our data highlighted firstly the ability of the $HgCl_2$-induced AKI to downregulate the expression of β3-AR to partake in the renal pathomechanisms of this metal since this negative impact correlated inversely with the elevated renal biomarkers. Besides activating the β3-AR, mirabegron has upregulated its gene expression, as well to concur with an earlier finding [27] in which the authors reported that, distinct from β1 and β2-ARs, the activation of the isotype β3 enhances its own transcription. To verify the dependence of mirabegron on the activation of β3-AR, blocking this receptor has re-escalated the kidney function parameters to mimic the effect of $HgCl_2$.

After binding to its receptor mirabegron modulated myriad factors that crosstalk to clarify its possible mechanism(s). Firstly, mirabegron by upregulating the expression of miR-127 explains its reno-therapeutic effect, where this miR was reported to defend proximal tubular cells against renal ischemia/reperfusion (I/R) injury through preservation of the cytoskeleton and TJ organization [28]. In the same milieu, it was

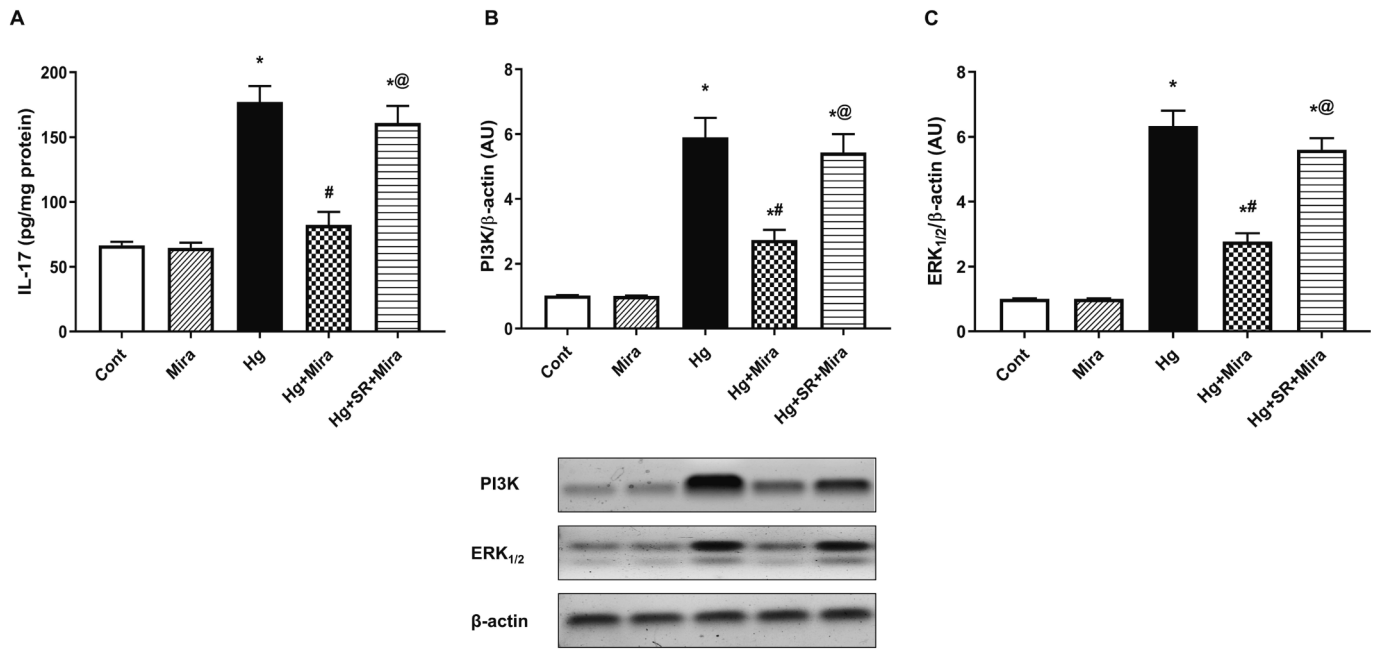

Fig. 5. Effect of Mira with or without SR59230A on renal content of (A) IL-17, and the protein expressions of (B) PI3K and (C) ERK½ in $HgCl_2$-induced AKI in rats. Results are presented as means ± SD (n = 6/3) and the one-way ANOVA followed by Tukey's Multiple Comparison tests was adopted to analyze the data statistically. As compared to Cont. (*), Hg ($^{\#}$), and Hg + Mira ($^{@}$)-treated group ($p < 0.05$). Mira was administered orally 1 and 24 hrs. after $HgCl_2$ subcutaneous injection, whereas the selective β3-AR blocker SR59230A was administered intraperitoneally 15 min. before each dose of Mira. β3-AR: beta 3 adrenergic receptor; Cont.: control, ERK½: extracellular signal-regulated kinase ½; Hg: mercuric chloride; IL-17: interleukin-17; Mira: mirabegron; PI3K: phosphoinositide 3-kinase; SR: SR59230A, a selective β3-AR antagonist.

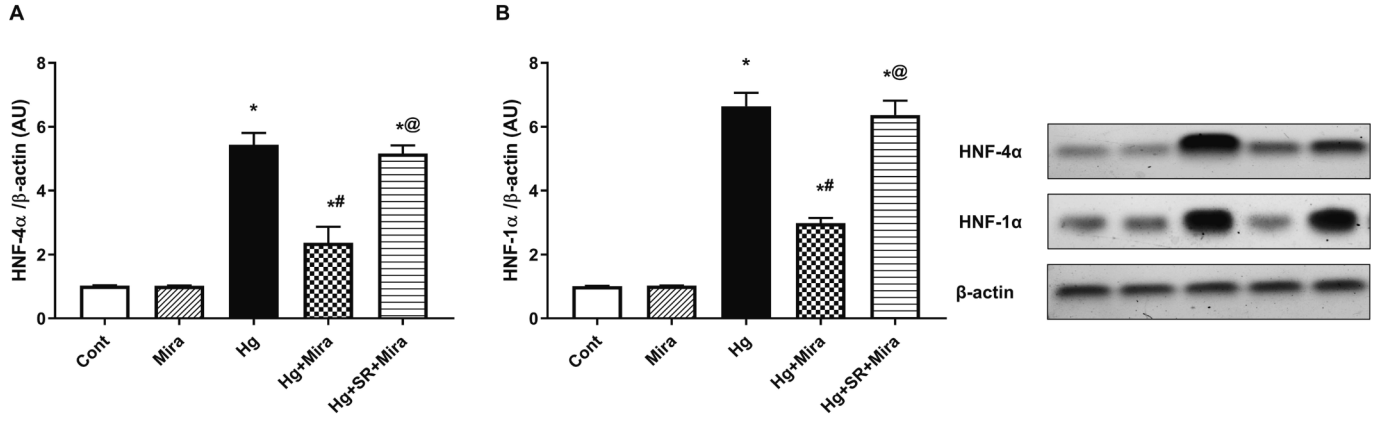

Fig. 6. Effect of Mira with or without SR59230A on renal protein expression of (A) HNF-4α and (B) HNF-1α in $HgCl_2$-induced AKI in rats. Results are presented as means ± SD (n = 3) and the one-way ANOVA followed by Tukey's Multiple Comparison tests was adopted to analyze the data statistically. As compared to Cont. (*), Hg ($^{\#}$), and Hg + Mira ($^{@}$)-treated group ($p < 0.05$). Mira was administered orally 1 and 24 hrs. after $HgCl_2$ subcutaneous injection, whereas the selective β3-AR blocker SR59230A was administered intraperitoneally 15 min. before each dose of Mira. β3-AR: beta 3 adrenergic receptor; Cont.: control, Hg: mercuric chloride; HNF: hepatocyte nuclear factor (-4α; −1α); Mira: mirabegron; SR: SR59230A, a selective β3-AR antagonist.

reported that the knockdown of miR-127 has aggravated the insult, a finding that can be extrapolated to the injurious effect of $HgCl_2$ which downregulated miR-127. This effect depends on the activation of β3-AR as proven herein in the blocker-treated group. Whether β-receptors can modulate the expression of different miRs has been proven in several aspects [29,30], however, the modulatory role of β3-AR on miR-127 to preserve kidney function is tested here for the first time.

In 2013, Park et al. [31] recounted the role of this non-coding mRNA in inhibiting inflammatory events justified by the suppression of NF-κB p65 and IL-1β to minimize catabolic effects in human chondrocytes. Thus, the upregulation of miR-127 in our study can be one cause of the anti-inflammatory capacity of mirabegron evinced herein by the suppressed protein expression of NF-κB p65, in a β3-AR-dependent manner, to participate in the improved kidney function. The provoked inflammatory events are considered critical features for the injurious role of $HgCl_2$ [32,33] and are intimately linked to renal disease. Although no data recounted the anti-inflammatory effect of β3-AR in the kidney, a previous study stated that activation of adrenergic β receptors using isoproterenol succeeded in reducing this transcription factor [34]. Additionally, we reported recently that the anti-colitic effect of mirabegron in an ulcerative colitis model involves the suppression of NF-κB p65 protein [18], results that back our current findings.

The suppressed NF-κB p65 by mirabegron entailed the cytokines IL-4, IL-13, and IL-17 but increased that of the anti-inflammatory cytokine IL-10. The beneficial role of IL-10 has been reported earlier in both ischemic and cisplatin-induced AKI [35] to support the present findings.

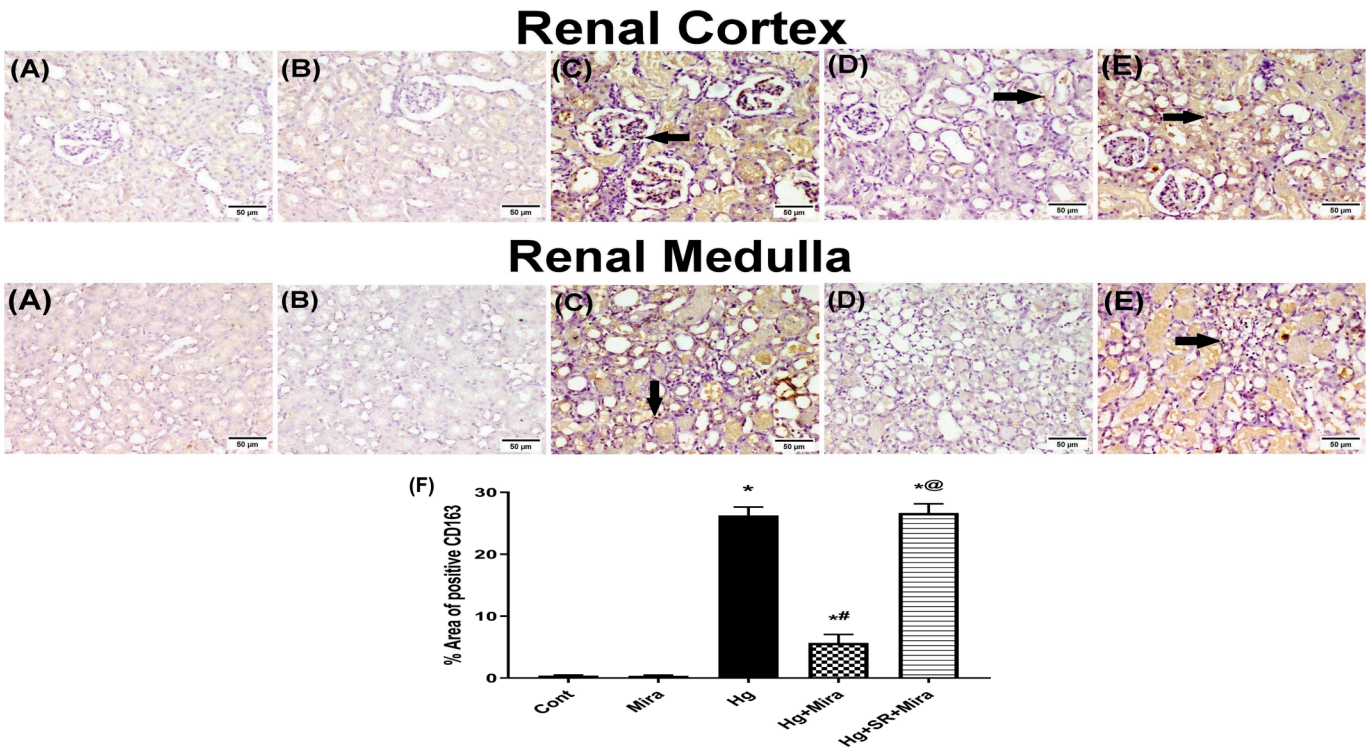

Fig. 7. Effect of Mira with or without SR59230A on renal CD-163 immunoreactivity in $HgCl_2$-induced AKI in rats. Compared to sections of (A) Cont. and (B) Mira, which show no protein expression, the section of (C) $HgCl_2$ reveals a high expression of this cluster. However, the section of (D) $HgCl_2$ + Mira depleted this expression, which was intensified again in the section of (E) $HgCl_2$ + SR59230A + Mira. Panel (F) depicts the percentage area of positive CD-163. Results are presented as means ± SD (n = 3) and the one-way ANOVA followed by Tukey's Multiple Comparison tests was adopted to analyze the data statistically. As compared to Cont. (*), Hg ($^{\#}$), and Hg + Mira ($^{@}$)-treated group ($p < 0.05$). Mira was administered orally 1 and 24 hrs. after $HgCl_2$ subcutaneous injection, whereas the selective β3-AR blocker SR59230A was administered intraperitoneally 15 min. before each dose of Mira. β3-AR: beta 3 adrenergic receptor; CD-163: cluster of differentiation 163; Cont.: control, Hg: mercuric chloride; Mira: mirabegron; SR: SR59230A, a selective β3-AR antagonist.

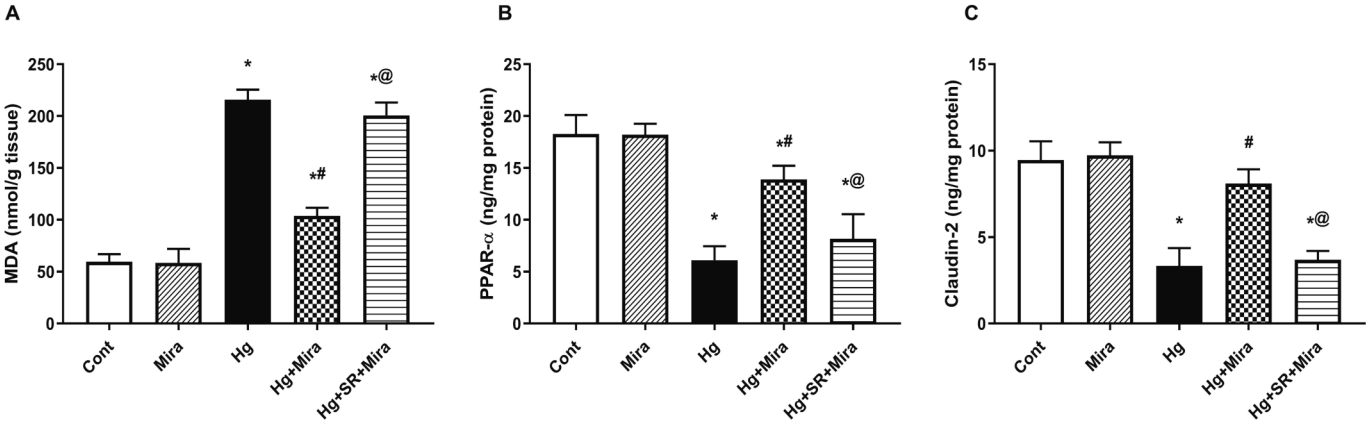

Fig. 8. Effect of Mira with or without SR59230A on renal contents of (A) MDA, (B) PPAR-α, and TJ (C) claudin-2 in $HgCl_2$-induced AKI in rats. Results are presented as means ± SD (n = 6/3) and the one-way ANOVA followed by Tukey's Multiple Comparison tests was adopted to analyze the data statistically. As compared to Cont. (*), Hg ($^{\#}$), and Hg + Mira ($^{@}$)-treated group ($p < 0.05$). Mira was administered orally 1 and 24 hrs. after $HgCl_2$ subcutaneous injection, whereas the selective β3-AR blocker SR59230A was administered intraperitoneally 15 min. before each dose of Mira. β3-AR: beta 3 adrenergic receptor; Cont.: control, Hg: mercuric chloride; MDA: malondialdehyde; Mira: mirabegron; PPAR-α: peroxisome proliferative activated receptor-alpha; SR: SR59230A, a selective β3-AR antagonist.

On the other hand, IL-4, −13, and −17 were part of the injurious players as reported here and *hitherto*, where exposure of the kidney to inorganic mercury increased IL-4 [36,37] and IL-17 [38] to perform a toxic role. In addition, elevated IL-4 is suggested as a predictor of cardiovascular events that are associated with chronic kidney disease (CKD) [39]. Moreover, the inflammatory cytokines IL-17 and IL-13 keep the inflammatory loop running since IL-17 is an inducer of IL-13, and both are considered upstream signaling molecules for NF-κB p65 [40,41].

Additionally, mirabegron leveled off STAT-6 which is a downstream target of the activated IL-17/IL-13 axis [42], and signaling through the IL-17/IL-13/STAT-6 trajectory is considered a crucial mechanism to the $HgCl_2$-induced AKI, a finding that matches earlier studies using models of polycystic kidney disease [43] and doxorubicin-induced AKI [44]. The latter authors tethered this signaling pathway with the induction of

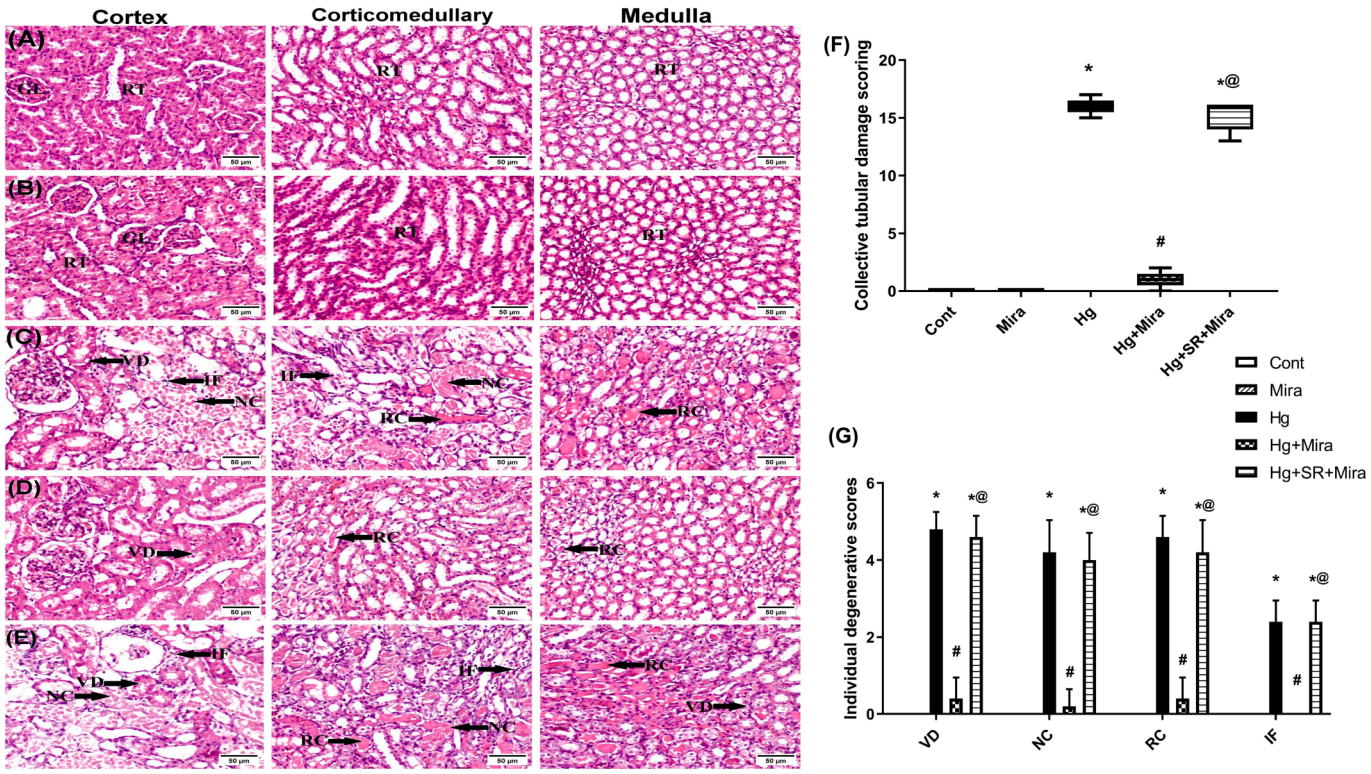

Fig. 9. Effect of Mira with or without SR59230A on renal histopathology in $HgCl_2$-induced AKI in rats. Photomicrographs representing H&E-stained renal cortex, corticomedullary junction, and renal medulla (X 200; scale bar 50 μm) show the normal histological characters of renal parenchyma, normal glomeruli (GL), and renal tubules (RT) in groups of (A) Cont. and (B) Mira. However, the epithelial lining of renal tubules from the section of (C) $HgCl_2$ depicts vacuolar degeneration (VD) and coagulative necrosis (NC), besides eosinophilic renal cast in the lumen of renal tubules (RC) and inflammatory cells infiltration (IF). Nevertheless, treatment with (D) Mira shows a marked improvement in the microscopic examination as verified by the slight VD of epithelium tubules, RC, and NC, effects that were canceled in the section of (E) $HgCl_2$ + SR25230A + Mira to resemble the alterations mediated by $HgCl_2$. Panels F and G demonstrated the score of collective and individual changes, respectively. Results are presented as median (min–max) (n = 3) and the Kruskal Wallis test, followed by the post-hoc Dunn's test was adopted to compare the different groups ($p < 0.05$). As compared to Cont. (*), Hg ($^{\#}$), and Hg + Mira ($^{@}$)-treated groups. Mira was administered orally 1 and 24 hrs. after $HgCl_2$ subcutaneous injection, whereas the selective β3-AR blocker SR59230A was administered intraperitoneally 15 min. before each dose of Mira. β3-AR: beta 3 adrenergic receptor; Cont.: control, Hg: mercuric chloride; Mira: mirabegron; SR: SR59230A, a selective β3-AR antagonist.

renal inflammatory response, oxidative stress, and cell apoptosis. Moreover, the currently increased IL-4 intersects with IL-13 and stimulates also STAT-6, where Dutta et al., [45] proved that IL-4 is also upstream of STAT-6.

Apart from being a major transcription factor of pro-inflammatory cytokines, NF-κB p65 is responsible for the activation of iNOS [46,47] to pose $HgCl_2$ nephrotoxicity [48] and kidney injury [49]. The current inhibitory effect of mirabegron on iNOS goes in line with that reported in experimental models of OUB [50]. This effect contributes to its beneficial role against $HgCl_2$, where mirabegron offered cardioprotection against angiotensin II insult by suppressing iNOS [51]. In the same milieu, the antioxidant potential of mirabegron, proven here by the inhibition of $HgCl_2$-induced lipid peroxidation and earlier in a colitic model [18] is another player that integrates with its anti-inflammatory role to interrupt the injurious vicious cycle tethering oxidative stress with inflammation. This fact has been addressed earlier, where Gonzalez [46] reported that in an in-vitro model, treatment of hepatocytes with IL-1β increased the transcription factor NF-κB p65 which in turn activated iNOS to consequently augment the overproduction of oxidative stress. Other participants in the inflammatory scene are $ERK_{1/2}$ and PI3K which were boosted in the $HgCl_2$ untreated group to assent with previous findings [52–54]. Moreover, the enhancement of $ERK_{1/2}$ and PI3K/Akt axis was reported to partake in the induction of NF-κB p65 [55] and the injurious impact of the signaling pathway IL-17/$ERK_{1/2}$/NF-κB p65 has been reported earlier in a cardio-injury model [56]. Thus, the mirabegron-mediated inhibition of the IL-17/$ERK_{1/2}$ axis and PI3K adds a further explanation for the suppressed NF-κB p65 and the quelling of the inflammatory progress.

We proved also that mirabegron has increased PPAR-α which is strongly expressed in the kidney [57] to match the earlier findings revealing that activation of β3-AR has upregulated the expression PPAR-α in a model of atherosclerosis [58]. The enhancement of this transcription factor can further elucidate the anti-inflammatory mechanism of mirabegron since it is known that PPAR-α interacts with NF-κB p65 to interfere with its DNA binding [59]. Moreover, this receptor crosstalk with the inflammatory cytokines, where it was reported that PPAR-α knockout mice had a higher level of IL-13 [60] and that the activated PPAR-α mediates an anti-inflammatory effect in IL-10 deficient mice with colitis by decreasing IL-17 [61] Additionally, the activation of PPAR-α by fenofibrate offered renoprotection by the repression of NF-κB [62].

Another novel finding reported herein is the mirabegron-induced downregulation of the protein expression of hepatocyte nuclear factors 1 alpha (HNF-1α) and HNF-4 and their upregulation after the $HgCl_2$ insult. Indeed, HNF-1α is a transcriptional activator whose activity is controlled by that of HNF-4α [63]. HNF-1α has been expressed in the liver, pancreas, and kidney [64] to mediate specific cellular functions and regulate targeting signals which are somehow addressed in the liver and pancreas but still ambiguous in the kidney [65]. The expression of the two transcriptional activators mainly in the proximal convoluted tubules is to maintain their physiological function and regulate renal trafficking and transportation [66]. Despite the protective role, our $HgCl_2$ insult has upregulated their protein expression, an effect that may be linked with the inflammatory events recalled herein. This concept can

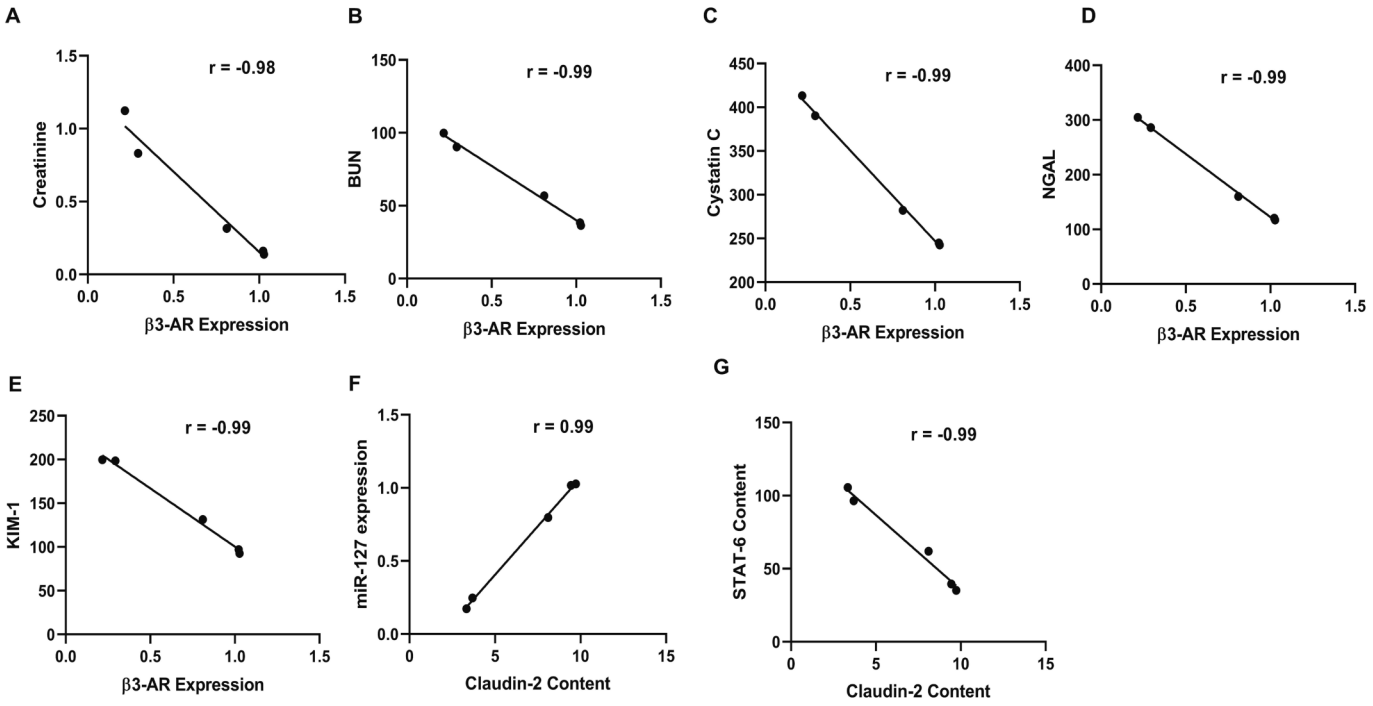

Fig. 10. Correlation between β3-AR and (A) creatinine, (B) BUN, (C) cystatin-C, (D) NGAL, and (E) KIM-1 as well as the correlation between the TJ claudin-2 with (F) miR-127 and (G) STAT-6 in $HgCl_2$-induced AKI in rats. Correlations for the measured parameters were carried out using Pearson's correlation test. Mira was administered orally 1 and 24 hrs. after $HgCl_2$ subcutaneous injection, whereas the selective β3-AR blocker SR59230A was administered intraperitoneally 15 min. before each dose of Mira. β3-AR: beta 3 adrenergic receptor; BUN: blood urea nitrogen; Cont.: control; Hg: mercuric chloride; KIM-1: kidney injury molecule-1; Mira: mirabegron; NGAL: neutrophil gelatinase-associated lipocalin; SR: SR59230A, a selective β3-AR antagonist, STAT-6: signal transducer and activator of transcription 6.

be upheld by the findings of Lin et al. [67] stating that the enhancement of HNF-1α activates NF-κB p65 and its trajectory to reduce the gene expression/replication of the hepatitis B virus. In the same concept, Sucajtys-Szulc et al. [68] owed the pro-inflammatory effect of HNF-1α in a model of CKD to the increased expression of NF-κB p65 and its downstream targets and concluded that HNF-1α can be upstream of NF-κB p65 in livers of patients with CKD. Regarding HNF-4, Gonzalez [46] proved that the IL-1β/NF-κB p65 axis-induced iNOS requires first the activation of HNF-4 to increase the link of HNF-4 to the iNOS promoter. Hence, the aptitude of mirabegron, by activating the β3-AR, to lessen HNF-1α and HNF-4 can adjoin to its anti-inflammatory role.

Besides the participation of the activated cytokines in the renal inflammatory process, the activation of resident macrophages, among other inflammatory cells, integrates to complete the inflammatory network. Although the pro-inflammatory cytokines are triggered simply following AKI, the response of the macrophages is over-simplification, where their ability to polarize from one phenotype to the other depends on their functional plasticity and their role in tissue injury and repair [69].

Our findings revealed a concomitant increment in the content/protein expression of the M1 phenotype markers (NF-κB p65, iNOS, IL-17), as well as those of M2 (IL-4, IL-13, CD163, STAT6, $ERK_{1/2}$) after the induction of AKI model. The post-administration of mirabegron, on the other hand, has leveled these markers off to be reactivated in the group of SR59230A, results that confirm the results of Hadi et al. [19], who recounted the expression of β3-AR in macrophages. Although it is commonly reported that under simple acute responses, M1 macrophages progress linearly to the M2 phase, however, in chronic conditions, both phenotypes may coexist [8], a recent study [70] pointed to the activation of the M2 phenotype in AKI. This effect may mediate a compensatory mechanism to abate the M1-induced inflammation and to heal the injured kidney [71,72] as abetted by the findings of Moeckel et al [7]. Despite the common beneficial role of M2, another study suggested the participation of the M2 cells in the inflammatory event by recruiting neutrophils after releasing certain chemokines [73]. In addition, other studies stated that activated M2 macrophages may provoke renal fibrosis apart from their amendment effects against injurious insults [74,75]. Therefore, the current co-existence of M1/M2 macrophages may result from the release of diverse signaling molecules resulting in a complex interconnected array of responses to enhance the activation of both phenotypes.

In a model of COPD, the ratio of M2/M1 was increased along with the PI3K/AKT axis to prove its role in the activation of M2 polarization [76]. Our findings, hence, coincide with the previous study, where the $HgCl_2$ insult has induced PI3K along with the activation of M2. Whether these increments favor the compensatory effect of activated M2 is yet to be clarified, since PI3K has accompanied kidney injury in different models including the inorganic mercury [53,54,77]. Another activator of the M2 polarization is STAT6, a regulator of IL-4-stimulated M2 macrophage [78]. Finally, activated $ERK_{1/2}$, a member of the mitogen-activated protein kinase (MAPK) signaling pathways, has been reported to play a pivotal role in promoting the survival of M1 macrophages in CKD [79]. Later, another study highlighted the role of this MAPK member in the stimulation of M2 polarization [80]. The $HgCl_2$-inducing effect on M1/M2-related markers besides PI3K, $ERK_{1/2}$, and STAT6 has been reversed by mirabegron to be re-enhanced upon using the β3-AR antagonist. In a previous study, Finlin et al. [81] indicated the ability of mirabegron to augment M2 markers ($CD163^+/CD68^+$) but not those of M1 ($CD86^+/CD68^+$) in inflamed adipose tissue of obese humans. Though this finding is partly opposite to our data, mirabegron here has succeeded to correct both the altered M1, as well as its markers. Moreover, the mirabegron-induced inhibition of the activated macrophages can be endowed to the activated PPAR-α, where this transcription factor is expressed in these cells [82,83] to function as an immunomodulator to suppress ROS and iNOS-mediated RNS released from M1 macrophages [84].

The last participant in the reno-therapeutic effect of mirabegron is claudin-2, a TJ expressed in the kidney mainly in the proximal tubules to govern cation and water permeability by acting as a leaky ion channel [10]. Treatment with mirabegron antagonized the $HgCl_2$ inhibitory effect and increased the renal content of claudin-2, an effect that depended on the stimulation of β3-AR. The beneficial role of the augmented TJ was recounted earlier against a renal I/R model, where the absence of claudin-2 aggravated the injurious effect of this insult [11]. The mirabegron stimulating effect is related to several factors; the upregulation of miR-127 can be the first reason behind the augmented claudin-2 as shown herein by the strong positive correlation between them. Previously, it was reported that this non-coding mRNA preserved kidney function by enhancing the organization of ZO-1, another TJ [28]. Moreover, the antioxidant and anti-inflammatory capacity of mirabegron besides the increased miR-127 [31], can be partly responsible for the enhanced claudin-2. Indeed, previous studies recounted that ROS and the inflammatory cascade decrease its formation [10,85]. Additionally, the mirabegron-induced suppression of NF-κB p65 and its upstream signals $ERK_{1/2}$ and PI3K/AKT [10,55] partakes in the restoration of claudin-2 as stated previously that signaling through $ERK_{1/2}$ pathway negatively regulates claudin-2 in the PCT [86]. In the same milieu, Naringenin, a flavanone that enhances the β-adrenergic agonist isoproterenol [87] was found to increase claudin-2 in Madin–Darby canine kidney II cell monolayers [88] and to mediate its anti-inflammatory and anti-oxidant effects against acute lung injury by inhibiting the PI3K/AKT pathways [89] to shed some light on the injurious role of the latter hub. Despite no research linked between renal STAT-6 and claudin-2, our results showed a strong negative relationship between both. However, in intestinal injurious models, a positive regulatory effect of STAT-6 on the expression of claudin-2 was recorded amply [90,91], a discrepancy that can be linked to the different organs used. Moreover, the inhibitory impact of mirabegron on the inflammatory cytokines IL-4, IL-13, and IL-17 cannot be ruled out, where they are chained with NF-κB p65 as targets and inducers and are considered upstream of STAT-6, $ERK_{1/2}$, and PI3K as mentioned earlier. The last effector studied herein is PPAR-α which parallels claudin-2 in the studied groups to concur with an earlier finding in an early diabetes-induced nephropathy model [92]. These authors reported a decrease in the two proteins in the nephropathic group and concluded that diabetes affects renal function and alters TJ besides PPAR-α.

To recapitulate our findings, we proved herein that mirabegron, depending on the activation of β3-AR, can be useful in treating the injurious effect of the nephron-toxicant $HgCl_2$. Mirabegron mediated its reno-therapeutic effect by the suppression of inflammatory cascades and oxidative stress, besides the activated M1/M2 macrophages. Additionally, mirabegron stimulated the beneficial factors, such as miR-127, PPAR-α, and the TJ claudin-2. These effects resulted from turning off several intersecting inflammatory trajectories as IL-17/$ERK_{1/2}$/NF-κB p65, IL-4 & IL-13/STAT-6; IL-4/ & IL-17/PI3K, IL-17/ERK½/NF-κB p65, HNF-4α/HNF-1α/NF-κB p65 that entailed also the suppression of the activated macrophage phenotypes. Hence, our data may nominate the repurposing of mirabegron in the treatment of $HgCl_2$-induced AKI and urge further examinations of the β3-AR agonist in other AKI models.

Funding

This research received no external funding.

CRediT authorship contribution statement

Mahmoud M. Kamal: Methodology, Resources, Validation, Writing – original draft, Data curation, Visualization. **Hanan S. El-Abhar:** Conceptualization, Data curation, Formal analysis, Supervision, Writing – review & editing. **Dalaal M. Abdallah:** . **Kawkab A. Ahmed:** . **Nour Eldin S. Aly:** . **Mostafa A Rabie:** .

Declaration of Competing Interest

The authors declare that they have no known competing financial interests or personal relationships that could have appeared to influence the work reported in this paper.

Data availability

Data will be made available on request.

References

[1] J.-D. Park, W. Zheng, Human exposure and health effects of inorganic and elemental mercury, J. Prev. Med. Public Health 45 (2012) 344–352, https://doi.org/10.3961/jpmph.2012.45.6.344.
[2] C.C. Bridges, R.K. Zalups, Transport of inorganic mercury and methylmercury in target tissues and organs, J. Toxicol. Environ. Health, Part B 13 (2010) 385–410, https://doi.org/10.1080/10937401003673750.
[3] M. Nava, F. Romero, Y. Quiroz, G. Parra, L. Bonet, B. Rodríguez-Iturbe, Melatonin attenuates acute renal failure and oxidative stress induced by mercuric chloride in rats, Am. J. Physiol.-Renal Physiol. 279 (2000) F910–F918, https://doi.org/10.1152/ajprenal.2000.279.5.F910.
[4] K. Suzuki, T. Kanabayashi, H. Nakayama, K. Doi, Kinetics of chemokines and their receptors in mercuric chloride-induced tubulointerstitial lesions in brown Norway rats, Exp. Mol. Pathol. 75 (2003) 58–67, https://doi.org/10.1016/S0014-4800(03)00028-5.
[5] F. Duthie, E.D. O'Sullivan, J. Hughes, I.S.N. Forefronts Symposium, The diverse function of macrophages in renal disease, Kidney Int. Rep. 1 (2016) (2015) 204–209, https://doi.org/10.1016/j.ekir.2016.08.004.
[6] Q. Cao, Y. Wang, D.C.H. Harris, Pathogenic and protective role of macrophages in kidney disease, Am. J. Physiol.-Renal Physiol. 305 (2013) F3–F11, https://doi.org/10.1152/ajprenal.00122.2013.
[7] G. Moeckel, M. Palmer, L. Cantley, A. Vichot, Quantification and localization of M2 macrophages in human kidneys with acute tubular injury, Int. J. Nephrol. Renovasc. Dis. (2014) 415. https://doi.org/10.2147/IJNRD.S66936.
[8] R.C. Landis, K.R. Quimby, A.R. Greenidge, M1/M2 macrophages in diabetic nephropathy: Nrf2/HO-1 as therapeutic targets, Curr. Pharm. Des. 24 (2018) 2241–2249, https://doi.org/10.2174/1381612824666180716163845.
[9] J. Hou, The kidney tight junction (review), Int. J. Mol. Med. 34 (2014) 1451–1457, https://doi.org/10.3892/ijmm.2014.1955.
[10] S. Venugopal, S. Anwer, K. Szászi, Claudin-2: roles beyond permeability functions, Int. J. Mol. Sci. 20 (2019) 5655, https://doi.org/10.3390/ijms20225655.
[11] L. Pei, G. Solis, M.T.X. Nguyen, N. Kamat, L. Magenheimer, M. Zhuo, J. Li, J. Curry, A.A. McDonough, T.A. Fields, W.J. Welch, A.S.L. Yu, Paracellular epithelial sodium transport maximizes energy efficiency in the kidney, J. Clin. Investig. 126 (2016) 2509–2518, https://doi.org/10.1172/JCI83942.
[12] G. Jacquillet, O. Barbier, M. Cougnon, M. Tauc, M.C. Namorado, D. Martin, J. L. Reyes, P. Poujeol, Zinc protects renal function during cadmium intoxication in the rat, Am. J. Physiol.-Renal Physiol. 290 (2006) F127–F137, https://doi.org/10.1152/ajprenal.00366.2004.
[13] K.a.d.f.e. ritz,, The sympathetic nervous system and the kidney: its importance in renal diseases, Blood Press. 7 (1998) 14–19, https://doi.org/10.1080/080370598438429.
[14] G. Procino, M. Carmosino, S. Milano, M. Dal Monte, G. Schena, M. Mastrodonato, A. Gerbino, P. Bagnoli, M. Svelto, β3 adrenergic receptor in the kidney may be a new player in sympathetic regulation of renal function, Kidney Int. 90 (2016) 555–567, https://doi.org/10.1016/j.kint.2016.03.020.
[15] G. Schena, M. Carmosino, S. Chiurlia, L. Onuchic, M. Mastropasqua, E. Maiorano, F.P. Schena, M.J. Caplan, β3 adrenergic receptor as potential therapeutic target in ADPKD, Physiol. Rep. 9 (2021). https://doi.org/10.14814/phy2.15058.
[16] L.Y.M. Michel, C. Farah, J.-L. Balligand, The Beta3 adrenergic receptor in healthy and pathological cardiovascular tissues, Cells. 9 (2020) 2584, https://doi.org/10.3390/cells9122584.
[17] N. Dehvari, E.D. da Silva Junior, T. Bengtsson, D.S. Hutchinson, Mirabegron: potential off target effects and uses beyond the bladder, Br. J. Pharmacol. 175 (2018) 4072–4082, https://doi.org/10.1111/bph.14121.
[18] S. Nasser, D.M. Abdallah, K.A. Ahmed, Y. Abdel-Mottaleb, H.S. El-Abhar, The novel anti-colitic effect of β-adrenergic receptors via modulation of PS1/BACE-1/Aβ axis and NOTCH signaling in an ulcerative colitis model, Front. Pharmacol. 13 (2022), https://doi.org/10.3389/fphar.2022.1008085.
[19] T. Hadi, R. Douhard, A.M.M. Dias, M. Wendremaire, M. Pezzè, M. Bardou, P. Sagot, C. Garrido, F. Lirussi, Beta3 adrenergic receptor stimulation in human macrophages inhibits NADPHoxidase activity and induces catalase expression via PPARγ activation, Biochim. Biophys. Acta (BBA) – Mol. Cell Res. 1864 (2017) 1769–1784, https://doi.org/10.1016/j.bbamcr.2017.07.003.
[20] A.-M.-M. Fouda, M.-H.-Y. Daba, G.M. Dahab, O.A. Sharaf el-Din, Thymoquinone ameliorates renal oxidative damage and proliferative response induced by mercuric chloride in rats, Basic Clin. Paharmacol. Toxicol. 103 (2008) 109–118, https://doi.org/10.1111/j.1742-7843.2008.00260.x.
[21] M.G. de Oliveira, J.A. Rojas-Moscoso, G.M. Bertollotto, T.Z. Candido, L.R. de A. Kiguti, A.S. Pupo, E. Antunes, G. de Nucci, F.Z. Mónica, Mirabegron elicits rat

corpus cavernosum relaxation and increases in vivo erectile response, Eur. J. Pharmacol. 858 (2019), 172447, https://doi.org/10.1016/j.ejphar.2019.172447.
[22] S. Bexis, J.R. Docherty, Role of α_1 - and β_3 -adrenoceptors in the modulation by SR59230A of the effects of MDMA on body temperature in the mouse, Br. J. Pharmacol. 158 (2009) 259–266, https://doi.org/10.1111/j.1476-5381.2009.00186.x.
[23] Y. Ootsuka, K. Kulasekara, R.C. de Menezes, W.W. Blessing, SR59230A, a beta-3 adrenoceptor antagonist, inhibits ultradian brown adipose tissue thermogenesis and interrupts associated episodic brain and body heating, Am. J. Physiol.-Regulatory, Integrative and Comparative Physiol. 301 (2011) R987–R994, https://doi.org/10.1152/ajpregu.00085.2011.
[24] O. Ernst, T. Zor, Linearization of the bradford protein assay, J. Vis. Exp. (2010), https://doi.org/10.3791/1918.
[25] S.K. Suvarna, C. Layton, J.D. Bancroft, Bancroft's theory and practice of histological techniques, Elsevier (2019), https://doi.org/10.1016/C2015-0-00143-5.
[26] S.M. Mansour, S.A. Abd El-Aal, H.S. El-Abhar, K.A. Ahmed, M.M. Awny, Repositioning of Ticagrelor: Renoprotection mediated by modulating renin-angiotensin system, inflammation, autophagy and galectin-3, Eur. J. Pharmacol. 918 (2022), 174793, https://doi.org/10.1016/j.ejphar.2022.174793.
[27] R.F. Thomas, B.D. Holt, D.A. Schwinn, S.B. Liggett, Long-term agonist exposure induces upregulation of beta 3-adrenergic receptor expression via multiple cAMP response elements., Proceedings of the National Academy of Sciences. 89 (1992) 4490–4494. https://doi.org/10.1073/pnas.89.10.4490.
[28] E. Aguado-Fraile, E. Ramos, D. Sáenz-Morales, E. Conde, I. Blanco-Sánchez, K. Stamatakis, L. del Peso, E. Cuppen, B. Brüne, M.L.G. Bermejo, miR-127 Protects Proximal Tubule Cells against Ischemia/Reperfusion: Identification of Kinesin Family Member 3B as miR-127 Target, PLoS One 7 (2012) e44305.
[29] C.J. Martyniuk, R. Martínez, D.J. Kostyniuk, J.A. Mennigen, J. Zubcevic, Genetic ablation of bone marrow beta-adrenergic receptors in mice modulates miRNA-transcriptome networks of neuroinflammation in the paraventricular nucleus, Physiol. Genomics 52 (2020) 169–177, https://doi.org/10.1152/physiolgenomics.00001.2020.
[30] F. Shi, S. Collins, Second messenger signaling mechanisms of the brown adipocyte thermogenic program: an integrative perspective, Horm. Mol. Biol. Clin. Investig. (2017), https://doi.org/10.1515/hmbci-2017-0062.
[31] S.J. Park, E.J. Cheon, M.H. Lee, H.A. Kim, MicroRNA-127-5p regulates matrix metalloproteinase 13 expression and interleukin-1β-induced catabolic effects in human chondrocytes, Arthritis Rheum. 65 (2013) 3141–3152, https://doi.org/10.1002/art.38188.
[32] S. Li, M. Shi, Y. Wan, Y. Wang, M. Zhu, B. Wang, Y. Zhan, B. Ran, C. Wu, Inflammasome/NF-κB translocation inhibition via PPARγ agonist mitigates inorganic mercury induced nephrotoxicity, Ecotoxicol. Environ. Saf. 201 (2020), 110801, https://doi.org/10.1016/j.ecoenv.2020.110801.
[33] C. Caglayan, F.M. Kandemir, S. Yildirim, S. Kucukler, G. Eser, Rutin protects mercuric chloride-induced nephrotoxicity via targeting of aquaporin 1 level, oxidative stress, apoptosis and inflammation in rats, J. Trace Elem. Med Biol. 54 (2019) 69–78, https://doi.org/10.1016/j.jtemb.2019.04.007.
[34] S.Z. Safi, H. Shah, R. Qvist, P. Bindal, M. Mansor, G.O.S. Yan, I.S.B. Ismail, Beta adrenergic receptors stimulation attenuates phosphorylation of NF-κB and IκBα in hyperglycemic endothelial cells, Cell. Physiol. Biochem. 51 (2018) 1429–1436, https://doi.org/10.1159/000495591.
[35] J. Deng, Y. Kohda, H. Chiao, Y. Wang, X. Hu, S.M. Hewitt, T. Miyaji, P. Mcleroy, B. Nibhanupudy, S. Li, R.A. Star, Interleukin-10 inhibits ischemic and cisplatin-induced acute renal injury, Kidney Int. 60 (2001) 2118–2128, https://doi.org/10.1046/j.1523-1755.2001.00043.x.
[36] J. Dastych, A. Walczak-Drzewiecka, J. Wyczolkowska, D.D. Metcalfe, Murine mast cells exposed to mercuric chloride release granule-associated N-acetyl-β-D-hexosaminidase and secrete IL-4 and TNF-α, J. Allergy Clin. Immunol. 103 (1999) 1108–1114, https://doi.org/10.1016/S0091-6749(99)70186-7.
[37] W. Coers, J.T.W.M. Vos, P.H. Van Der Meide, M.L.C. Van Der Horst, S. Huitema, J. J. Weening, Interferon-gamma (IFN-γ) and IL-4 expressed during mercury-induced membranous nephropathy are toxic for cultured podocytes, Clin. Exp. Immunol. 102 (2008) 297–307, https://doi.org/10.1111/j.1365-2249.1995.tb03781.x.
[38] R.M. Gardner, J.F. Nyland, E.K. Silbergeld, Differential immunotoxic effects of inorganic and organic mercury species in vitro, Toxicol. Lett. 198 (2010) 182–190, https://doi.org/10.1016/j.toxlet.2010.06.015.
[39] L. Gu, H. Liu, X. Liu, X. Zeng, Z. Lei, X. Wan, The relationship between interleukin-4 levels and cardiovascular events in patients with chronic kidney disease, Risk Manag Healthc Policy 13 (2020) 2371–2377, https://doi.org/10.2147/RMHP.S270845.
[40] K. Goto, Y. Chiba, M. Misawa, IL-13 induces translocation of NF-κB in cultured human bronchial smooth muscle cells, Cytokine 46 (2009) 96–99, https://doi.org/10.1016/j.cyto.2008.12.021.
[41] S. Xie, J. Li, J.H. Wang, Q. Wu, P. Yang, H.-C. Hsu, L.E. Smythies, J.D. Mountz, IL-17 activates the canonical NF-κB signaling pathway in autoimmune B cells of BXD2 mice to upregulate the expression of regulators of G-protein signaling 16, J. Immunol. 184 (2010) 2289–2296, https://doi.org/10.4049/jimmunol.0903133.
[42] S.L. Hall, T. Baker, S. Lajoie, P.K. Richgels, Y. Yang, J.W. McAlees, A. van Lier, M. Wills-Karp, U. Sivaprasad, T.H. Acciani, T.D. LeCras, J.B. Myers, M.B. Kovacic, I.P. Lewkowich, IL-17A enhances IL-13 activity by enhancing IL-13–induced signal transducer and activator of transcription 6 activation, J. Allergy Clin. Immunol. 139 (2017) 462–471.e14, https://doi.org/10.1016/j.jaci.2016.04.037.
[43] E.E. Olsan, J.D. West, J.A. Torres, N. Doerr, T. Weimbs, Identification of targets of IL-13 and STAT6 signaling in polycystic kidney disease, Am. J. Physiol.-Renal Physiol. 315 (2018) F86–F96, https://doi.org/10.1152/ajprenal.00346.2017.
[44] Q. Zhang, G. Wu, S. Guo, Y. Liu, Z. Liu, Effects of tristetraprolin on doxorubicin (adriamycin)-induced experimental kidney injury through inhibiting IL-13/STAT6 signal pathway, Am. J. Transl. Res. 12 (2020) 1203–1221.
[45] A.K. Dutta, K. Boggs, A. Khimji, Y. Getachew, Y. Wang, C. Kresge, D.C. Rockey, A. P. Feranchak, Signaling through the interleukin-4 and interleukin-13 receptor complexes regulates cholangiocyte TMEM16A expression and biliary secretion, Am. J. Physiol.-Gastrointestinal and Liver Physiol. 318 (2020) G763–G771, https://doi.org/10.1152/ajpgi.00219.2019.
[46] F.J. Gonzalez, Role of HNF4α in the superinduction of the IL-1β-activated iNOS gene by oxidative stress, Biochem. J 394 (2006), https://doi.org/10.1042/BJ20060005.
[47] F. Zhang, Y.L. Siow, K. o, Hyperhomocysteinemia activates NF-κB and inducible nitric oxide synthase in the kidney, Kidney Int. 65 (2004) 1327–1338, https://doi.org/10.1111/j.1523-1755.2004.00510.x.
[48] A. Stacchiotti, F. Ricci, R. Rezzani, G.L. Volti, E. Borsani, A. Lavazza, R. Bianchi, L. F. Rodell, Tubular stress proteins and nitric oxide synthase expression in rat kidney exposed to mercuric chloride and melatonin, J. Histochem. Cytochem. 54 (2006) 1149–1157, https://doi.org/10.1369/jhc.6A6932.2006.
[49] J. Zhang, R.P. Brown, M. Shaw, V.S. Vaidya, Y. Zhou, P. Espandiari, N. Sadrieh, M. Stratmeyer, J. Keenan, C.G. Kilty, J.V. Bonventre, P.L. Goering, Immunolocalization of Kim-1, RPA-1, and RPA-2 in kidney of gentamicin-, mercury-, or chromium-treated rats: relationship to renal distributions of iNOS and nitrotyrosine, Toxicol. Pathol. 36 (2008) 397–409, https://doi.org/10.1177/0192623308315832.
[50] O. Iatsyna, S. Vernygorodskyi, F. Kostyev, Morphological assessment of no-synthase distribution in overactive bladder and stress urine incontinence in animal models administered with experimental pharmacocorrection regimens, Georgian Med News. (2018) 143–150.
[51] J.-R. Lin, L.-L.-Q. Ding, L. Xu, J. Huang, Z.-B. Zhang, X.-H. Chen, Y.-W. Cheng, C.-C. Ruan, P.-J. Gao, Brown adipocyte ADRB3 mediates cardioprotection via suppressing exosomal iNOS, Circ. Res. 131 (2022) 133–147, https://doi.org/10.1161/CIRCRESAHA.121.320470.
[52] A. Aguado, M. Galán, O. Zhenyukh, G.A. Wiggers, F.R. Roque, S. Redondo, F. Peçanha, A. Martín, A. Fortuño, V. Cachofeiro, T. Tejerina, M. Salaices, A. M. Briones, Mercury induces proliferation and reduces cell size in vascular smooth muscle cells through MAPK, oxidative stress and cyclooxygenase-2 pathways, Toxicol. Appl. Pharmacol. 268 (2013) 188–200, https://doi.org/10.1016/j.taap.2013.01.030.
[53] M.O. Kadry, R.M. Abdel Megeed, Ubiquitous toxicity of mercuric chloride in target tissues and organs: Impact of Ubidecarenone and liposomal-Ubidecarenone STAT 5A/ PTEN /PI3K/AKT signaling pathways, J. Trace Elem. Med Biol. 74 (2022), 127058, https://doi.org/10.1016/j.jtemb.2022.127058.
[54] B. Liu, S. Ao, F. Tan, W. Ma, H. Liu, H. Liang, X. Yang, X. Chi, Transcriptomic analysis and laboratory experiments reveal potential critical genes and regulatory mechanisms in sepsis-associated acute kidney injury, Ann Transl Med. 10 (2022) 737–737. https://doi.org/10.21037/atm-22-845.
[55] W. Liu, S. Huang, Y. Li, Y. Li, D. Li, P. Wu, Q. Wang, X. Zheng, K. Zhang, Glycyrrhizic acid from licorice down-regulates inflammatory responses *via* blocking MAPK and PI3K/Akt-dependent NF-κB signalling pathways in TPA-induced skin inflammation, Medchemcomm. 9 (2018) 1502–1510, https://doi.org/10.1039/C8MD00288F.
[56] Y. Liu, H. Zhu, Z. Su, C. Sun, J. Yin, H. Yuan, S. Sandoghchian, Z. Jiao, S. Wang, H. Xu, IL-17 contributes to cardiac fibrosis following experimental autoimmune myocarditis by a PKCβ/Erk1/2/NF-κB-dependent signaling pathway, Int. Immunol. 24 (2012) 605–612, https://doi.org/10.1093/intimm/dxs056.
[57] S.A. Kliewer, B.M. Forman, B. Blumberg, E.S. Ong, U. Borgmeyer, D.J. Mangelsdorf, K. Umesono, R.M. Evans, Differential expression and activation of a family of murine peroxisome proliferator-activated receptors., Proceedings of the National Academy of Sciences. 91 (1994) 7355–7359. https://doi.org/10.1073/pnas.91.15.7355.
[58] S. Shi, Y. Li, Y. Guo, Z. Wang, Effect of beta-3 adrenoceptor stimulation on the levels of ApoA-I, PPARα, and PPARγ in apolipoprotein e–deficient mice, J. Cardiovasc. Pharmacol. 64 (2014) 407–411, https://doi.org/10.1097/FJC.0000000000000133.
[59] N. Zhang, E.S.H. Chu, J. Zhang, X. Li, Q. Liang, J. Chen, M. Chen, N. Teoh, G. Farrell, J.J.Y. Sung, J. Yu, Peroxisome proliferator activated receptor alpha inhibits hepatocarcinogenesis through mediating NF-κB signaling pathway, Oncotarget 5 (2014) 8330–8340. https://doi.org/10.18632/oncotarget.2212.
[60] G. Woerly, K. Honda, M. Loyens, J.-P. Papin, J. Auwerx, B. Staels, M. Capron, D. Dombrowicz, Peroxisome proliferator–activated receptors α and γ down-regulate allergic inflammation and eosinophil activation, J. Exp. Med. 198 (2003) 411–421, https://doi.org/10.1084/jem.20021384.
[61] J.W. Lee, P.J. Bajwa, M.J. Carson, D.R. Jeske, Y. Cong, C.O. Elson, C. Lytle, D. S. Straus, Fenofibrate represses interleukin-17 and interferon-γ expression and improves colitis in interleukin-10–deficient mice, Gastroenterology 133 (2007) 108–123, https://doi.org/10.1053/j.gastro.2007.03.113.
[62] N. Zuo, X. Zheng, H. Liu, X. Ma, Fenofibrate, a PPARα agonist, protect proximal tubular cells from albumin-bound fatty acids induced apoptosis via the activation of NF-kB, Int. J. Clin. Exp. Path. 8 (2015) 10653–10661.
[63] S.K. Hansen, M. Párrizas, M.L. Jensen, S. Pruhova, J. Ek, S.F. Boj, A. Johansen, M. A. Maestro, F. Rivera, H. Eiberg, M. Andel, J. Lebl, O. Pedersen, J. Ferrer, T. Hansen, Genetic evidence that HNF-1α–dependent transcriptional control of HNF-4α is essential for human pancreatic β cell function, J. Clin. Investig. 110 (2002) 827–833, https://doi.org/10.1172/JCI15085.

[64] H.H. Lau, N.H.J. Ng, L.S.W. Loo, J.B. Jasmen, A.K.K. Teo, The molecular functions of hepatocyte nuclear factors – In and beyond the liver, J. Hepatol. 68 (2018) 1033–1048, https://doi.org/10.1016/j.jhep.2017.11.026.
[65] J.W. Chan, C.W.Y. Neo, S. Ghosh, H. Choi, S.C. Lim, E.S. Tai, A.K.K. Teo, HNF1A binds and regulates the expression of SLC51B to facilitate the uptake of estrone sulfate in human renal proximal tubule epithelial cells, Cell Death Dis. 14 (2023) 302, https://doi.org/10.1038/s41419-023-05827-8.
[66] H. Saito, Pathophysiological regulation of renal SLC22A organic ion transporters in acute kidney injury: Pharmacological and toxicological implications, Pharmacol. Ther. 125 (2010) 79–91, https://doi.org/10.1016/j.pharmthera.2009.09.008.
[67] J. Lin, C. Gu, Z. Shen, Y. Liu, W. Wang, S. Tao, X. Cui, J. Liu, Y. Xie, Hepatocyte nuclear factor 1α downregulates HBV gene expression and replication by activating the NF-κB signaling pathway, PLoS One 12 (2017) e0174017.
[68] E. Sucajtys-Szulc, A. Debska-Slizien, B. Rutkowski, M. Szolkiewicz, J. Swierczynski, R.T. Smolenski, Hepatocyte nuclear factor 1α proinflammatory effect linked to the overexpression of liver nuclear factor–κB in experimental model of chronic kidney disease, Int. J. Mol. Sci. 23 (2022) 8883, https://doi.org/10.3390/ijms23168883.
[69] H.I. Han, L.B. Skvarca, E.B. Espiritu, A.J. Davidson, N.A. Hukriede, The role of macrophages during acute kidney injury: destruction and repair, Pediatr. Nephrol. 34 (2019) 561–569, https://doi.org/10.1007/s00467-017-3883-1.
[70] X. Meng, J. Jin, H.Y. Lan, Driving role of macrophages in transition from acute kidney injury to chronic kidney disease, Chin. Med. J. (Engl.) 135 (2022) 757–766, https://doi.org/10.1097/CM9.0000000000002100.
[71] K. Singbartl, C.L. Formeck, J.A. Kellum, Kidney-immune system crosstalk in AKI, Semin. Nephrol. 39 (2019) 96–106, https://doi.org/10.1016/j.semnephrol.2018.10.007.
[72] V. Andrade-Oliveira, O. Foresto-Neto, I.K.M. Watanabe, R. Zatz, N.O.S. Câmara, Inflammation in renal diseases: new and old players, Front. Pharmacol. 10 (2019), https://doi.org/10.3389/fphar.2019.01192.
[73] Q. Hu, C.J. Lyon, J.K. Fletcher, W. Tang, M. Wan, T.Y. Hu, Extracellular vesicle activities regulating macrophage- and tissue-mediated injury and repair responses, Acta Pharm. Sin. B 11 (2021) 1493–1512, https://doi.org/10.1016/j.apsb.2020.12.014.
[74] M.A. Vernon, K.J. Mylonas, J. Hughes, Macrophages and renal fibrosis, Semin. Nephrol. 30 (2010) 302–317, https://doi.org/10.1016/j.semnephrol.2010.03.004.
[75] G.J. Ko, C.-S. Boo, S.-K. Jo, W.Y. Cho, H.K. Kim, Macrophages contribute to the development of renal fibrosis following ischaemia/reperfusion-induced acute kidney injury, Nephrol. Dial. Transplant. 23 (2007) 842–852, https://doi.org/10.1093/ndt/gfm694.
[76] J. Lu, L. Xie, C. Liu, Q. Zhang, S. Sun, PTEN/PI3k/AKT regulates macrophage polarization in emphysematous mice, Scand. J. Immunol. 85 (2017) 395–405, https://doi.org/10.1111/sji.12545.
[77] L. Meng, L. Li, S. Lu, K. Li, Z. Su, Y. Wang, X. Fan, X. Li, G. Zhao, The protective effect of dexmedetomidine on LPS-induced acute lung injury through the HMGB1-mediated TLR4/NF-κB and PI3K/Akt/mTOR pathways, Mol. Immunol. 94 (2018) 7–17, https://doi.org/10.1016/j.molimm.2017.12.008.
[78] S. Wang, C. Zhang, J. Li, S. Niyazi, L. Zheng, M. Xu, R. Rong, C. Yang, T. Zhu, Erythropoietin protects against rhabdomyolysis-induced acute kidney injury by modulating macrophage polarization, Cell Death Dis. 8 (2017) e2725–e, https://doi.org/10.1038/cddis.2017.104.
[79] E.T. Richardson, S. Shukla, N. Nagy, W.H. Boom, R.C. Beck, L. Zhou, G.E. Landreth, C.V. Harding, ERK signaling is essential for macrophage development, PLoS One 10 (2015) e0140064.
[80] T. Neamatallah, Mitogen-activated protein kinase pathway: A critical regulator in tumor-associated macrophage polarization, J. Microsc. Ultrastruct. 7 (2019) 53, https://doi.org/10.4103/JMAU.JMAU_68_18.
[81] B.S. Finlin, H. Memetimin, B. Zhu, A.L. Confides, H.J. Vekaria, R.H. El Khouli, Z. R. Johnson, P.M. Westgate, J. Chen, A.J. Morris, P.G. Sullivan, E.E. Dupont-Versteegden, P.A. Kern, The β3-adrenergic receptor agonist mirabegron improves glucose homeostasis in obese humans, J. Clin. Investig. 130 (2020) 2319–2331, https://doi.org/10.1172/JCI134892.
[82] V.R. Babaev, H. Ishiguro, L. Ding, P.G. Yancey, D.E. Dove, W.J. Kovacs, C. F. Semenkovich, S. Fazio, M.F. Linton, Macrophage expression of peroxisome proliferator-activated receptor-α reduces atherosclerosis in low-density lipoprotein receptor-deficient mice, Circulation 116 (2007) 1404–1412, https://doi.org/10.1161/CIRCULATIONAHA.106.684704.
[83] G. Chinetti, J.-C. Fruchart, B. Staels, Peroxisome proliferator-activated receptors: new targets for the pharmacological modulation of macrophage gene expression and function, Curr. Opin. Lipidol. 14 (2003) 459–468, https://doi.org/10.1097/00041433-200310000-00006.
[84] F. Penas, G.A. Mirkin, M. Vera, Á. Cevey, C.D. González, M.I. Gómez, M.E. Sales, N. B. Goren, Treatment in vitro with PPARα and PPARγ ligands drives M1-to-M2 polarization of macrophages from T. cruzi-infected mice, Biochim. Biophys. Acta (BBA) - Mol. Basis Dis. (1852 (2015)) 893–904, https://doi.org/10.1016/j.bbadis.2014.12.019.
[85] L. Rosas-Martínez, R. Rodríguez-Muñoz, M. del C. Namorado-Tonix, F. Missirlis, L. del Valle-Mondragón, A. Sánchez-Mendoza, J.L. Reyes-Sánchez, L.G. Cervantes-Pérez, Hyperglycemic levels in early stage of diabetic nephropathy affect differentially renal expression of claudins-2 and -5 by oxidative stress, Life Sci. 268 (2021) 119003. https://doi.org/10.1016/j.lfs.2020.119003.
[86] J.H. Lipschutz, S. Li, A. Arisco, D.F. Balkovetz, Extracellular signal-regulated kinases 1/2 control claudin-2 expression in madin-darby canine kidney strain I and II cells, J. Biol. Chem. 280 (2005) 3780–3788, https://doi.org/10.1074/jbc.M408122200.
[87] J. Bae, Y. Yang, X. Xu, J. Flaherty, H. Overby, K. Hildreth, J. Chen, S. Wang, L. Zhao, Naringenin, a citrus flavanone, enhances browning and brown adipogenesis: Role of peroxisome proliferator-activated receptor gamma, Front. Nutr. 9 (2022), https://doi.org/10.3389/fnut.2022.1036655.
[88] M. Nakashima, M. Hisada, N. Goda, T. Tenno, A. Kotake, Y. Inotsume, I. Kameoka, H. Hiroaki, Opposing effect of naringenin and quercetin on the junctional compartment of MDCK II cells to modulate the tight junction, Nutrients 12 (2020) 3285, https://doi.org/10.3390/nu12113285.
[89] M. Zhao, C. Li, F. Shen, M. Wang, N. Jia, C. Wang, Naringenin ameliorates LPS-induced acute lung injury through its anti-oxidative and anti-inflammatory activity and by inhibition of the PI3K/AKT pathway, Exp. Ther. Med. 14 (2017) 2228–2234, https://doi.org/10.3892/etm.2017.4772.
[90] M.J. Rosen, R. Chaturvedi, M.K. Washington, L.A. Kuhnhein, P.D. Moore, S. S. Coggeshall, E.M. McDonough, J.-H. Weitkamp, A.B. Singh, L.A. Coburn, C. S. Williams, F. Yan, L. Van Kaer, R.S. Peebles, K.T. Wilson, STAT6 deficiency ameliorates severity of oxazolone colitis by decreasing expression of claudin-2 and Th2-inducing cytokines, J. Immunol. 190 (2013) 1849–1858, https://doi.org/10.4049/jimmunol.1201373.
[91] V. Domazetovic, T. Iantomasi, A.G. Bonanomi, M. Stio, Vitamin D regulates claudin-2 and claudin-4 expression in active ulcerative colitis by p-Stat-6 and Smad-7 signaling, Int. J. Colorectal Dis. 35 (2020) 1231–1242, https://doi.org/10.1007/s00384-020-03576-0.
[92] L. Rosas, R. Rodríguez, M. Carmen Namorado, J.L. Reyes, L.G. Cervantes, Characterization of claudin-5, -2, occludin and PPAR alpha in a model of early diabetic nephropathy, FASEB J. 33 (2019), https://doi.org/10.1096/fasebj.2019.33.1_supplement.567.14.